Facultat de Química Tarragona

UNIVERSITAT ROVIRA i VIRGILI

THE UNIVERSITY OF ARIZONA

BACHELOR'S THESIS:

Synthesis and Characterization of PACAP23 glycopeptides for improved stability and transport

Student: Daniel Varela Guerrero

Academic tutor: Mª Elena Fernández Gutiérrez

Professional tutor: Robin Polt

Bachelor's Degree in Chemistry

Course 2020-2021

TABLE OF CONTENTS

1. SUMMARY

In this thesis I want to discuss how the presence of a carbohydrate can improve the stability and the blood-brain barrier transport of $PACAP_{23}$, and how these properties differ by using different carbohydrates.

$PAPAC_{38}$ and $PACAP_{27}$ are endogenous peptides which have been studied for their neuroprotective properties against neurodegenerative diseases. Recently, it was studied if an easier to make version could also present these properties, and the results showed that $PACAP_{23}$ was the shortest bioactive compound.

Despite its positive effects, peptides present a series of drawbacks, apart from the difficulty in crossing the BBB for most compounds. Glycosylation has proved effective to help with these difficulties. Because of that, the success in the synthesis of a glycosylated $PACAP_{23}$ could open a wide range of possibilities in the design of a drug meant for the treatment of these diseases. The whole Experimental part of this Thesis will be carried out in Dr. Robin Polt's research group, at the University of Arizona.

A aquesta tesi vull parlar sobre com la presència d'un carbohidrat pot millorar l'estabilitat i el transport per la blood-brain barrier del $PACAP_{23}$, i com aquests valors poden variar segons el carbohidrat que s'utilitzi a l'estructura.

El $PACAP_{38}$ i el $PACAP_{27}$ són pèptids endogènics que s'han estudiat per les seves propietats neuroprotectores contra malalties neurodegeneratives. Recentment, s'ha estudiat si una versió més fàcil de preparar podria presentar aquestes propietats, essent $PACAP_{23}$ el pèptid més curt amb bioactivitat.

Tot i els seus efectes positius, els pèptids presenten alguns inconvenients, també tenint en compte la dificultat per creuar la BBB. S'ha demostrat que la glicòlisi és efectiva contra aquests problemes. Per això, l'èxit en la síntesi d'un compost glicosilat de $PACAP_{23}$ obriria un ventall de possibilitats pel desenvolupament de tractament per aquestes malalties. La part experimental del treball es realitzarà al grup de recerca del Dr. Robin Polt, a la University of Arizona.

2. OBJECTIVE

The objective of this bachelor's thesis is to synthesize and characterize four glycosylated $PACAP_{23}$ compounds. The difference between these compounds lies in the carbohydrate used in the glycosylation step of the synthesis, all of them will contain a different carbohydrate motif.

After that, the four compounds will be characterized by HPLC and mass spectrometry (ESI-MS) to check the correct obtention of the peptide. In affirmative case, the compounds will be used for *in vitro* and *in vivo* studies to measure their stability and blood-brain barrier penetration values. Because of the long periods of time needed for both studies, this data cannot be provided in this thesis, but the purity and characterization assessments will be discussed.

3. THEORETICAL PART

To fully understand the research carried out for the $PACAP_{23}$ glycopeptides, first it is important to introduce the current situation of neurodegenerative diseases, and the different scientific perspectives and research studies that make this project important for the development of a useful treatment for these types of pathologies.

3.1. PRESENT AND FUTURE IN THE TRATMENT OF NEURODEGERATIVE DISORDERS

From the last decades, neurodegenerative disorders such as Parkinson's disease and Alzheimer's disease have been a growing and expanding phenomenon for their ability to cause disability and death in the older adult population. These syndromes have become a significant issue, especially in the increasingly aging society predominant nowadays in western industrialized countries.

These disorders include complex molecular mechanisms, which involve inflammation and apoptosis, ultimately leading in progressive and severe neuronal loss. These facts have emphasized the need of a vast research effort to develop therapeutic remedies, like anti-inflammatory, free radical scavengers, or sodium and calcium channel blockers.

However, this effort has not resulted in the discovery of any treatment for such pathologies, and all current treatments are still palliative, for example in the case of Parkinson's disease, where the loss of dopamine in patients has to be compensated by different means, such as increasing the available dopamine level or by dopamine replacement.

Despite the apparent lack of success, some innovative projects have been carried out exhibited promising results that could lead to slow the process or even stop the symptoms [1][2].

3.2. PACAP: AN INNOVATIVE DRUG

One of the current research tendencies is the use of naturally present endogenous molecules. Inside this group of compounds, we find PACAP (pituitary adenylate cyclase-activating polypeptide).

As said above, PACAP is an endogenous C-terminally amidated peptide formed by 38 amino acids ($PACAP_{38}$). $PACAP_{27}$, a shorter analog of PACAP is also present in nature, consisting in 27 residues formed by an amidation producing an internal cleavage site in Gly^{28} -Lys^{29} -Arg^{30} residues of $PACAP_{38}$. An important remark to be made is that both PACAP38 and PACAP27 can activate the PAC_1, $VPAC_1$ and $VPAC_2$ receptors, a branch of the Secretin family of GPCRs (G protein-coupled receptors), also called class B GPCRs. $PACAP_{38}$ has higher

receptor affinity than $PACAP_{27}$, but both analogues are able to activate them with equal potency [2].

Table 1. Amino acid sequences of $PACAP_{38}$, $PACAP_{27}$, VIP, and Glucagon.

Compound	Amino Acid Sequence
$PACAP_{38}$	HSDGIFTDSYSRYRKQMAVKKYLAAVLGKRYKQRVKNK
$PACAP_{27}$	HSDGIFTDSYSRYRKQMAVKKYLAAVL
VIP	HSDAVFTDNYTRLRKQMAVKKYLNSILN
Glucagon	HSQGTFTSDYSKYLDSRRAQDFVQWLMNT

The closest homologue molecule to PACAP is VIP (or vasoactive intestinal peptide), a compound consisting of 28 amino acids. As seen in Table 1, VIP shares a 68% of its structure with PACAP. This is also seen by the fact that VIP can also activate the same receptors as PACAP: in the case of $VPAC_1$ and $VPAC_2$ the activation is similar to PACAP, but its ability to activate PAC_1 receptor is a thousand times lower than PACAP [2]. Its similarity with VIP identifies PACAP as a member the same superfamily also formed by GHRH, glucagon, PHM, GIP, among other substances.

Actually, it is presumed that the active part of the PACAP sequence has been conserved during evolution for more than 300 million years, and 26 of the 38 amino acids of its structure have been found in 16 different animal species, demonstrating the preservation and the importance of PACAP [3]. During numerous studies, PACAP has shown a big number of different biological functions. Some of them are the regulation of hormones from the hypothalamus, a strong vasodilator agent for some muscle cells [4], a bronchodilation promoter [5], and even a tumor growth controller.

3.2.1. IMMUNITY AND THERAPEUTICAL PROPERTIES OF PACAP

During the last years, a large number of studies (both *in vitro* and *in vivo*) have proved the promising therapeutic potential of PACAP in the treatment of cell death and neuroinflammation, typical symptoms of neurodegenerative diseases.

PACAP activity against neuronal apoptosis

Some studies have proved the ability of PACAP to block or slow neuron cell death in various *in vitro* cell systems triggered by different toxic molecules, inhibiting neuronal degeneration caused by various *in vivo* models of brain lesions. This remarkable fact indicates that PACAP and its derivatives could be key in the medical treatment of not only neurodegenerative diseases, but also ischemia and post-traumatic lesions [6].

The PACAP cell death protection effect is based in the inhibition of caspase-3, an enzyme responsible of the catalytic cleavage of important proteins, which results in cell apoptosis. As caspase-3 is also the most predominant caspase involved in the elevated neuronal death in Alzheimer's disease, it has become a target for medical research and one of the reasons PACAP has a high therapeutic

potential [7]. PACAP acts through the activation of PAC_1 receptor, which activates $G\alpha_s$ signaling, and, following the cAMP/PKA pathway shown in Figure 1, leads to the increase in Bcl-2 expression (B-cell lymphoma 2). This regulator protein hinders the release of cytochrome C, a small hemeprotein whose inhibition stops the activation of caspase-9, ultimately blocking caspase-3 activation. This helps maintaining mitochondrial stability preventing the release of these compounds [6, 9].

It is also important to mention that PACAP can also hinder potassium channels, which also blocks the release of TEA (triethanolamine), inhibiting caspase-3 activation by a different mechanism and preventing induced cell apoptosis [8].

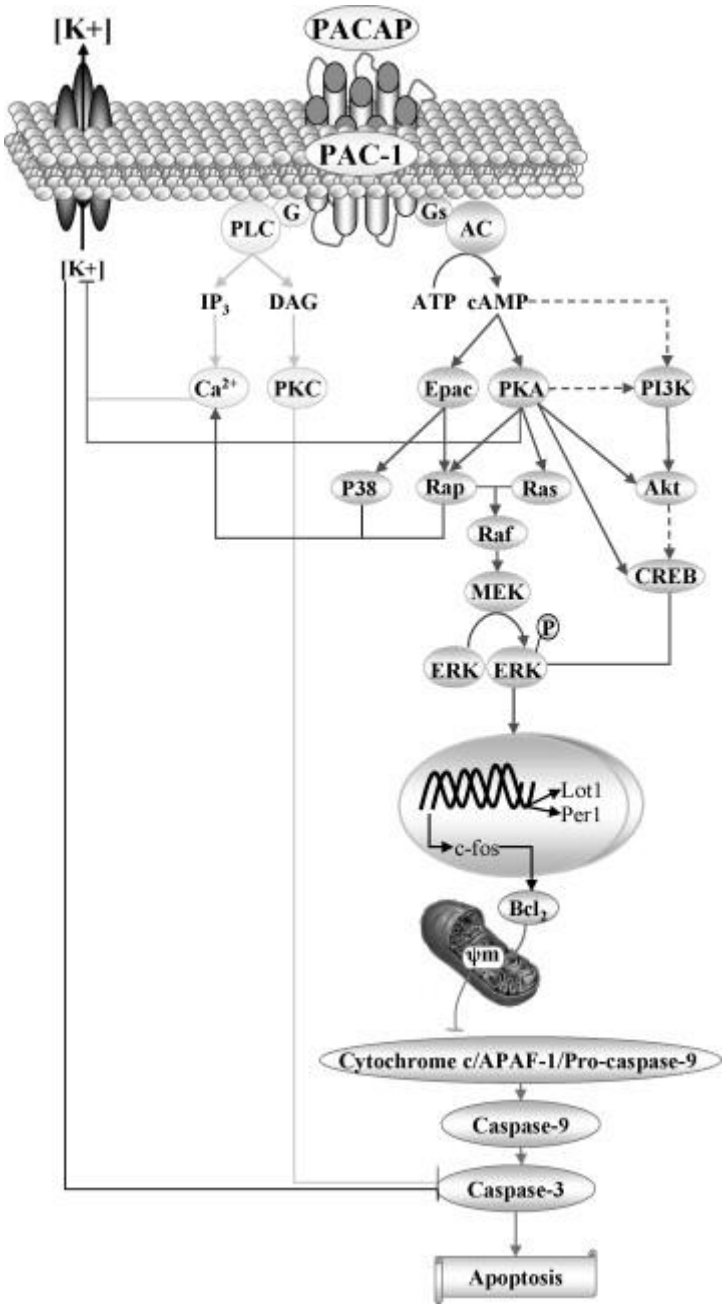

Figure 1. Scheme of the PACAP activity through the cAMP/PKA signaling pathway for caspase-3 inhibition [9].

Not only does PACAP protect neurons from apoptosis, but it also promotes neuron growth and development, known as neurotrophic factors. To do this, PACAP enables the expression and release of various neurotrophins (a family of proteins that favor neuron survival), in particular NGF (nerve growth factor), neurotrophin-1, neurotrophin-3, neurotrophin-4, BDNF (brain-derived neurotrophic factor). Moreover, PACAP also helps increasing the expression of ADNP (activity-dependent neurotrophic protein), an important protein for brain development and cognitive function, and whose levels decrease with Alzheimer's disease [2, 11].

Anti-inflammatory properties of PACAP

Brain inflammation is a regular defense strategy against toxic substances, infection and lesions. However, the effect of neurodegenerative diseases like Parkinson's disease, Alzheimer's disease or ALS, disturb the activation of microglia and the release of cytokines. This leads to the alteration of the equilibrium between pro-inflammatory and anti-inflammatory response due to the increase of inflammatory cytokines. The sustained inflammatory response ultimately leads to neuronal loss and neurodegeneration [12].

Another important property of PACAP is its ability to modulate this inflammatory response. PACAP has the ability to hinder the release of pro-inflammatory cytokines TNF-α (tumor necrosis factor α) and IL-1β (Figure 2). It has also been studied the inhibition in the production of NO and in the inhibition of NADHP oxidase (reducing the appearance of reactive oxygen species, ROS). Finally, PACAP induce the expression of anti-inflammatory cytokines IL-4 and IL-10.and stimulates the release of IL-6 (cytokine interleukin-6), enabling the alternative activation of macrophages, which help in the anti-inflammatory response [2, 13].

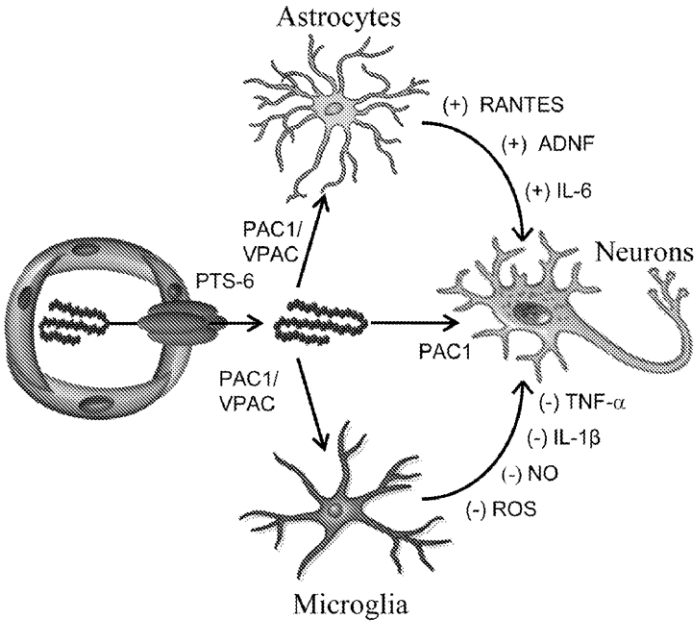

Figure 2. Direct and indirect effects of PACAP in the CNS to prevent neuronal death [2].

3.2.2. RESEARCH ON $PACAP_{23}$

After discussing the positive influence of PACAP in the central nervous system, some research projects were carried out to see if a truncated version of $PACAP_{27}$ could also functional and have an agonist effect, since a shorter version of the peptide would be more straightforward to produce and also more economic (Table 2). In order to investigate this possibility, peptides from $PACAP_{23}$ to $PACAP_{19}$ have been synthetized and tested to measure their activity and affinity with the three target receptors: PAC_1, $VPAC_1$, and $VPAC_2$. The results showed that $PACAP_{19}$, $PACAP_{20}$, $PACAP_{21}$ and $PACAP_{22}$ were unable to provide acceptable activity and affinity results. On the other hand, from $PACAP_{26}$ to $PACAP_{23}$, positive results were obtained, stating that $PACAP_{23}$ was the shortest biologically active peptide [1, 14].

Table 2. Amino acid sequences of PACAP38, PACAP27, and $PACAP_{23}$.

Compound	Amino Acid Sequence
$PACAP_{38}$	**HSDGIFTDSYSRYRKQMAVKKYLAAVLGKRYKQRVKNK**
$PACAP_{27}$	**HSDGIFTDSYSRYRKQMAVKKYLAAVL**
$PACAP_{23}$	**HSDGIFTDSYSRYRKQÑAVKKYL**

The conclusion of the research, as seen in Table 3, showed that $PACAP_{23}$ is an agonist compound with less affinity for PAC_1 than the other PACAP isoforms, with a higher affinity for $VPAC_1$ than $PACAP_{27}$, but with inability to bind to the $VPAC_2$ receptor. The decrease in affinity with the PAC_1 receptor compared to $PACAP_{27}$ can be explained by the partial loss of the α-helix conformation of the peptide due to the truncation of the 4 last amino acids from the C-terminal, because of the fact that α-helix conformation is important for optimal PAC_1 interaction. This suggests that residues from 24 to 27 are key to $VPAC_2$ affinity while also improves the affinity with PAC_1 and strains the interaction with $VPAC_1$.

Table 3. Binding affinity of PACAP forms on human PAC_1, $VPAC_1$ and $VPAC_2$ receptors [1].

	PAC1		VPAC1		VPAC2	
	IC_{50} (nM)[e]	pIC_{50}[f]	IC_{50} (nM)[e]	pIC_{50}[f]	IC_{50} (nM)[e]	pIC_{50}[f]
PACAP38	4.6 (2.7–7.7)	8.34 ± 0.11	3.6 (2.2–5.7)	8.45 ± 0.09	18 (4–78)	7.74 ± 0.28
PACAP27	9.1 (4.6–17.8)	8.04 ± 0.14	138 (41–458)	6.86 ± 0.25	131 (50–339)	6.88 ± 0.20
PACAP23	675 (228–1998)	6.75 ± 0.23	32 (19–55)	7.49 ± 0.12	$> 10^{-5}$	< 5

As discussed before, most of the neuroprotective action of PACAP is achieved through the PAC_1 receptor. Despite the decrease in the interaction of $PACAP_{23}$ with PAC_1, the peptide still shows strong neuroprotective effects and helps with neuronal cell survival. The study stated that $PACAP_{23}$ protected cells from toxic substances like glutamate, with a potency superior to $PACAP_{27}$ and similar to $PACAP_{38}$, confirming its promising properties and opening another branch of investigation to use PACAP as a medical treatment [1].

3.3. THE BLOOD-BRAIN BARRIER

For any medical agent meant to treat neurodegenerative diseases to develop its therapeutic function, they have to act inside the central nervous system (CNS) and the brain. In order to enter the CNS, these drugs must first go through the Blood-brain barrier (or BBB).

The Blood-brain barrier consists in structure formed by aggregates of tight junctions between the cells that form the inner surface of the walls of the cerebral blood vessels perfusing the brain (called endothelial membranes or endothelium) [15]. The structure of the blood-brain barrier only allows the selective diffusion of compounds to the brain, reaching an average extension of between 150 and 200 cm^2. These tight junctions are exclusive of the brain, with other blood vessels in the body not having any additional system with similar uses, allowing for some small compounds to flow by passive diffusion [16]. Other differences between normal endothelial cells and the ones composed in the BBB are that the latter possess a higher number of mitochondria and undergoes minimal pinocytosis activity (endocytic process in which small compounds enter a cell through invagination of its surface) [17].

As shown in Figure 2 and Figure 3, brain capillaries and the blood-brain barrier are supported and by glial brain cells, specifically the end-foot of astrocyte cells, which also assists in its maintenance [19]. Furthermore, the exterior surface of the endothelial cells is surrounded by a basement surface and pericyte cells, which are key in the functionality of the BBB.

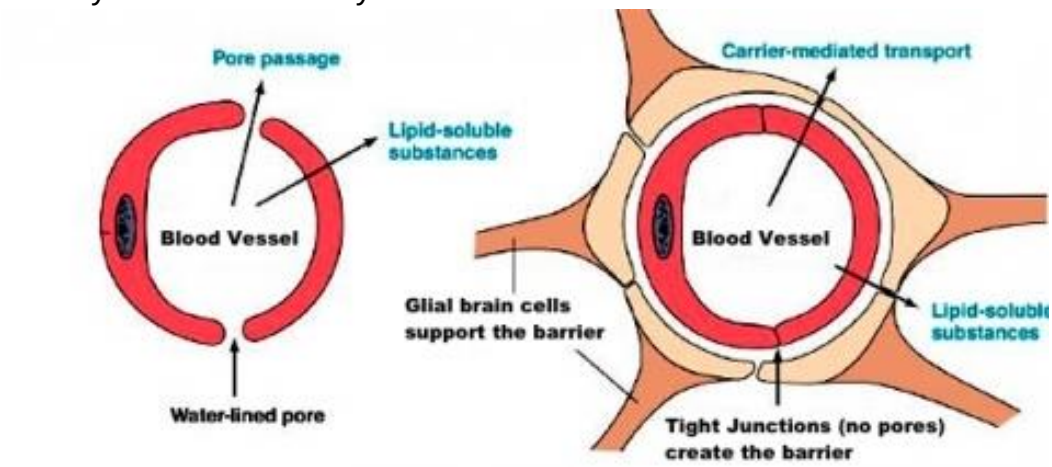

Figure 2. Schematic comparison of the cross sections of a normal blood vessel (left) and a brain blood vessel surrounded by the BBB (right) [18].

Pericytes help in the formation of the tight junctions and also inhibiting the immunity cells of the CNS and decreasing the presence of substances that could increase the barrier permeability [20, 21]. As can be seen in Figure 3, all these components including the microglia (responsible of the immunity defense of the brain), and the neurons form the Neurovascular Unit (NVU), whose main function is to detect the neuronal needs and provide them by vasodilation or vasoconstriction of the brain capillaries (functional hyperaemia) [22].

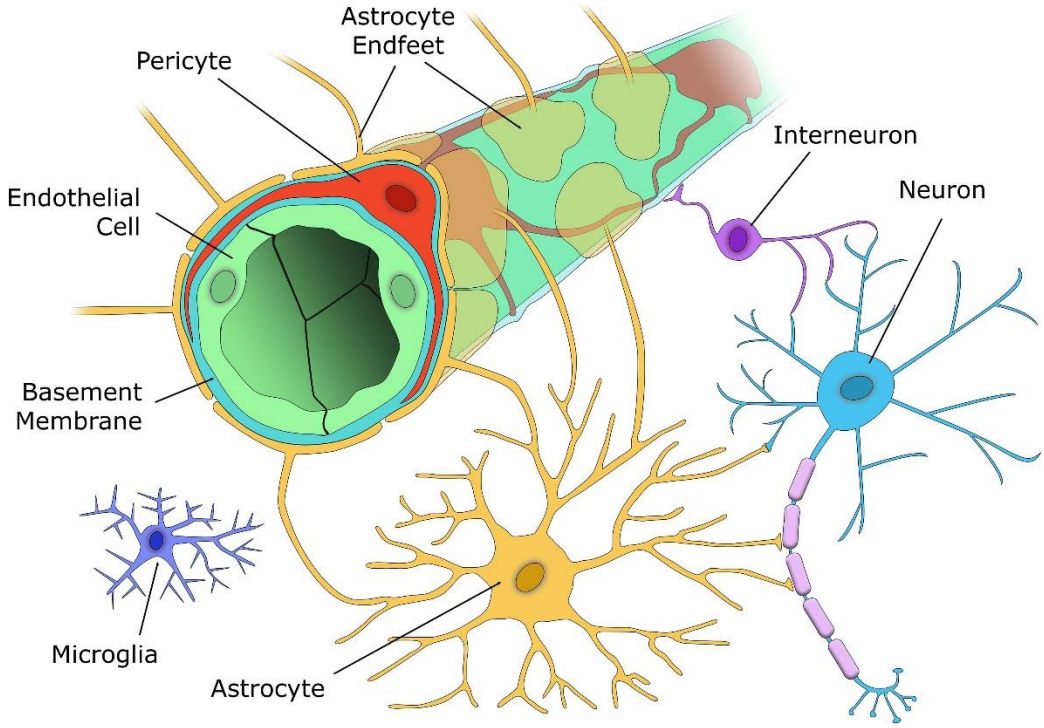

Figure 3. Representation of the components of the Neurovascular Unit (NVU) [21].

The main function of the blood-brain barrier is to prevent any toxic substances that can damage the brain from penetrating in the central nervous system by working as an additional boundary before reaching the brain. The BBB is highly selective, only allowing the flow of some essential compounds from the blood to the brain. Doing so, this structure protects the CNS from toxins from pathogens, toxic molecules, neurotransmitters such as glutamate or any substance that can potentially damage the brain in any manner with its presence or if a determined compound concentration is too high. Due to this, only water, certain gases (as oxygen), and lipid-soluble compounds can easily enter across the barrier. Other necessary substances like glucose can also pass through the barrier with some effort [15].

Another important purpose of this barrier is its function in the ion composition regulation of the central nervous system. Moreover, it has been observed that the BBB also acts as an interface having responsibility in the development of different nutritional, communicative, and homeostatic functions.

3.3.1. Crossing the Blood-Brain Barrier

It has been already stated that a compound that could possibly act as a treatment for neurodegenerative diseases must travel first trough the blood-brain barrier. Because of the high selectivity of the BBB, it is very difficult for most of these substances to cross it and reach the central nervous system. Because of this, the problem that encases crossing the barrier to deliver the drug to the brain has become the main obstacle in the designing of CNS drugs [23].

Some of the factors taken into account regarding blood-brain barrier transport are the molecular size, the chemical sequestration and the bioavailability and biostability of the designed compound.

As can be seen in Figure 4, the histamine tinted the organs and tissues of the animal, but not the brain and the spinal cord, which remain uncolored. The explanation of this is that histamine, a small molecule of about 110 Da can easily pass through the pores of the normal blood vessels but fails to enter the CNS due to the blood-brain barrier. This both demonstrates the protective function of the BBB and that opposed to previous thinking, small molecules do not cross the barrier without trouble.

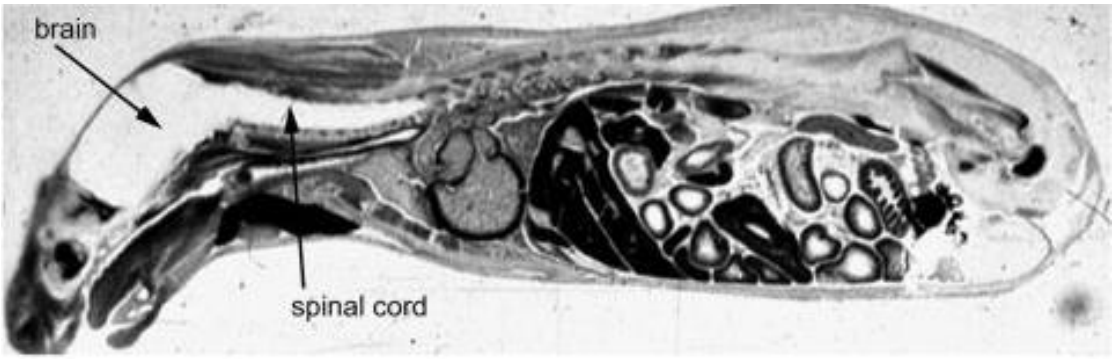

Figure 4. Autoradiogram of a sacrificed mouse 30 minutes after the injection of radiolabeled histamine [24].

Even though it was believed that small molecules could cross the BBB more easily, some research has showed that close to 98% of the compounds with a molecular mass under 400 Da (considered small compounds) do not easily pass through it [24].

In fact, it is known that as more than 98% of small molecules do not cross the BBB, almost 100% of large molecules including drugs cannot cross the barrier either. Despise this fact, less than 1% of the pharmaceutical companies and research projects in this field center its efforts in easing transport across the blood-brain barrier, being this one of the factors behind the lower drug development success rate targeting the central nervous system compared to other medical research areas.

These facts prove that size is not the determining factor for reaching the brain, but rather it is more important to ensure that the physiochemical properties of the designed therapeutical compound are adequate for transport through the BBB [23].

Centering in the physiochemical properties necessary to enter the blood-brain barrier, because of the lipid cell membrane part of the endothelial cells, compounds with higher lipid solubility (lipophilic or even amphiphilic substances) have an easier time crossing the BBB. Due to that, researchers have targeted the designing of drugs with improved lipid solubility, but considering that just

increasing it can affect solubility and bioavailability of the compound, also making the probability of plasma protein binding grow, decreasing the drug efficiency.

3.4. PEPTIDE GLYCOSYLATION

Peptides are a good option for creating drugs because of their high selectivity and potency. Another advantage of peptides is their rapid elimination of the body, which lowers the risk of toxicity, preventing its accumulation in tissues and organs. This instability can also be a problem in the case a long treatment is need. Some other drawbacks due to its peptide nature are that its bioavailability is low, and that the substance distribution is sometimes deficient. Based on its ability to cross the BBB and its neuroprotective properties, PACAP is still considered a good candidate for a future treatment for neurodegenerative diseases.

Taking into account both advantages and disadvantages of PACAP, some projects have been carried out, seeking to synthesize a PACAP derivative employing certain chemical modifications or conjugation of the peptide to another macromolecule, with the objective of maintaining its therapeutical properties while improving its stability and transport across the BBB. From all the methods studied, PACAP glycosylation has shown encouraging results for the designing a favorable drug.

Glycosylation consists in the covalent addition of a carbohydrate to another compound, in this case a peptide chain. Glycosylation is not unusual in the human body, being carried out to some extent in about half of the proteins contained in a cell. It is especially important in the secretory pathway, which involves the Golgi apparatus, the endoplasmic reticulum, and the vesicles that help release expressed proteins outside the cell. [25]

3.4.1. Effect of Glycosylation in PACAP stability

The low stability of PACAP (it usually has a circulating t½ of some minutes) is caused by DPP-IV (dipeptidyl peptidase-IV), a membrane associated enzyme which also affects other members of the PACAP-glucagon superfamily: glucose-dependent insulinotropic polypeptide (GIP) and glucagon-like peptide-1 (GLP-1). The action of DPP-IV is based in the cleavage of the 2 first amino acids from the N-terminal of the peptide, highly reducing its activity with the receptors (leaves PACAP3-27 and then PACAP5-27 fragments in the case of PACAP27). It is worth mentioning that the additional 11 amino acids of PACAP38 in the C-terminal (PACAP28-38) can interact with the enzyme, meaning that PACAP27 has less interaction with DPP-IV [26]. Glycosylation helps improve stability of the peptide by acting as an “steric shield” for molecules that can interact with PACAP and degrade it, as in the case of the DPP-IV enzyme.

O-linked glycosylation through the N-terminal has proven useful to hinder the activity of DPP-IV, but since the N-terminal is crucial for receptor activation, it can

reduce the efficacy of the drug, so C-terminal glycosylation has been set as the optimal position for binding. Although it has been theorized that glycosylation can cause partial loss of the α-helix conformation of the peptide (which as discussed before can reduce the affinity with PAC_1 receptor), some studies have demonstrated that the addition of a carbohydrate does not alter the structure of the peptide excessively, being more important the change in the peptide sequence than the addition or not of a carbohydrate. Furthermore, it has been stated that when a specific conformation is needed, a case-by-case study needs to be carried out for each designed glycopeptide to confirm its efficacy [27, 28].

3.4.2. Effect of Glycosylation on PACAP transport

It is believed that polycationic peptides can cross the blood-brain barrier using an adsorptive mediated transcytosis mechanism (Figure 5). This method consists in the association of a peptide with an average positive charge with the negatively charged endothelial membrane, which produces an invagination of the membrane resulting in a vesicle that crosses the membrane. After that, the vesicle reintegrates with the opposite side of the membrane (the abluminal side), delivering the peptide to the brain [28].

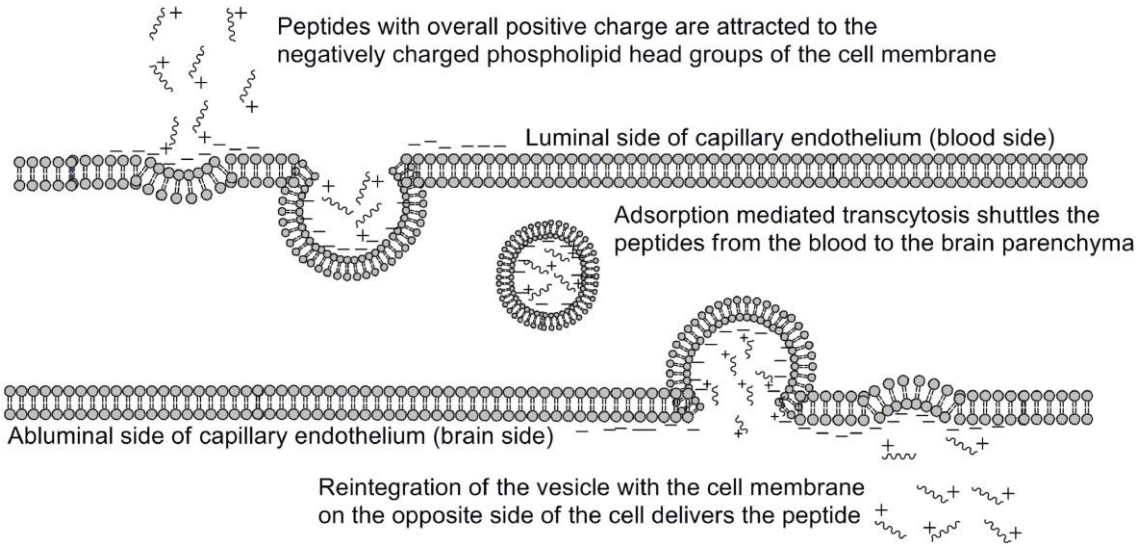

Figure 5. BBB penetration by adsorptive mediated transcytosis [28].

To find the receptor, peptides perform a search through the membrane. As can be seen in Figure 6, a peptide like PACAP presents a random coil structure until reaching the membrane, when it adopts a helical conformation. With this structure, the peptide interacts with the membrane to find its target receptor, testing that the “message sequence” of the peptide match the receptor. If it is not the correct receptor, the peptide returns to the aqueous medium recovering its previous random conformation, and the process is repeated along the membrane. There is an equilibrium between these two phases, creating a “hoping” effect in the membrane until the target receptor is found (Figure 7). This

process can be altered by alteration of the peptide structure with methods like glycosylation.

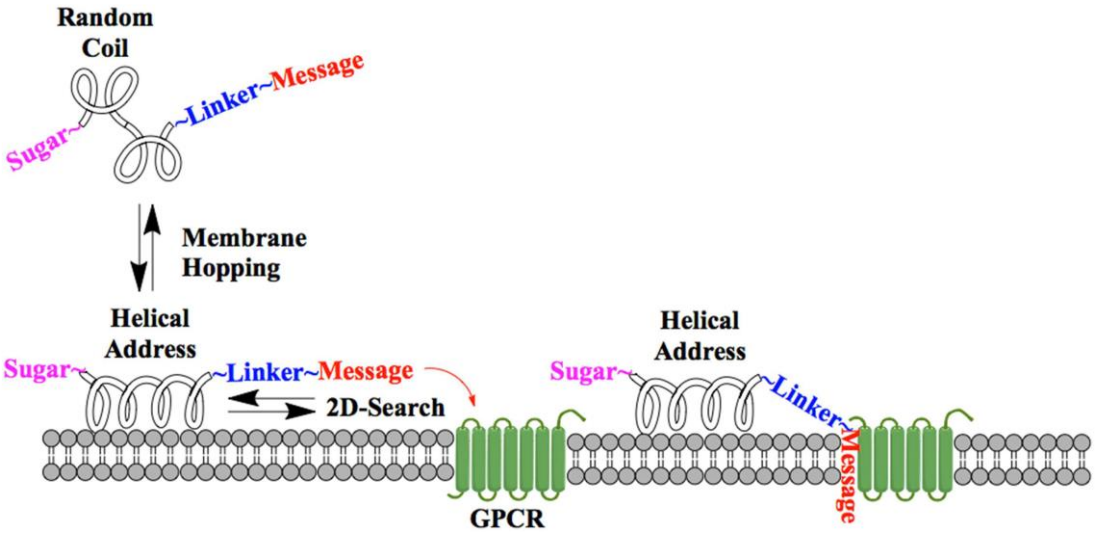

Figure 6. Representation of the interaction between the glycopeptide and the membrane and the change in the peptide conformation [28].

The addition of a carbohydrate regulates the amphipaticity of PACAP, being a crucial aspect of its functionality, as this allows to control its interaction and compatibility with biological membranes like the blood-brain barrier. The addition of a carbohydrate moiety means adding a polar region in the PACAP structure, decreasing the lipophilicity, (adding a disaccharide instead of a monosaccharide amplifies the effect). This change makes the glycopeptide have a higher affinity towards the aqueous environment (and the random coil conformation), leading to the reduction of the time binding to receptors and the time spent in the membrane, as the BBB is a lipophilic membrane.

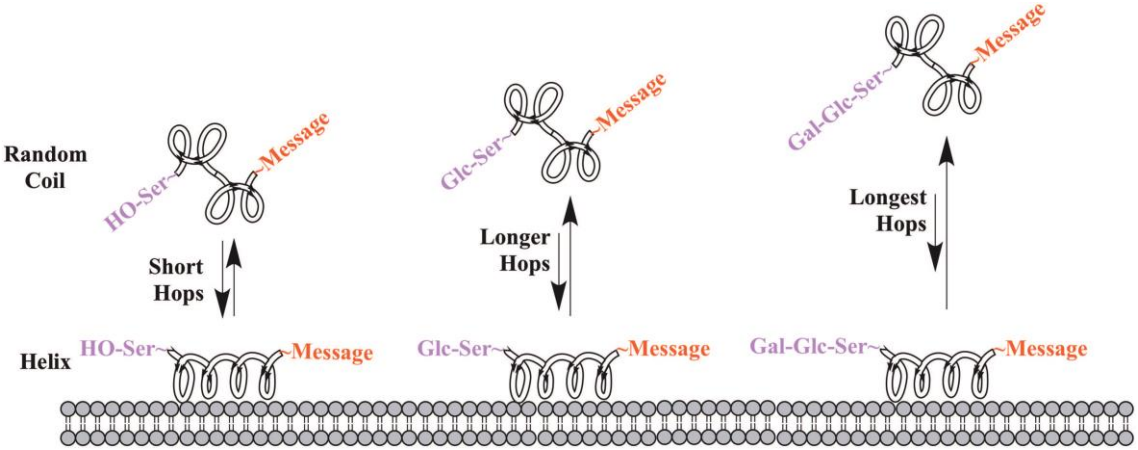

Figure 7. Membrane "hopping" mechanism of the glycopeptide in the membrane. The change of compounds in the C-terminal cause an increase in the effect [28].

Even though favoring the aqueous environment may seem negative, the reality is that glycosylation improves the bioavailability and the blood-brain barrier penetration. This happens due to the fact that the increased hydrophilicity also

induces an increase in the "hopping" effect because it is easier for the peptide to leave the membrane when the receptor does not match, simplifying the search, and ultimately increasing the probability of finding the correct receptor [27, 28].

To evaluate the beneficial aspects of glycolysis in peptide transport, a study carried out by the University of Arizona, the University of New England, and the University of Rochester Medical Center, designed an experiment in which would be measured how the presence and the type of carbohydrate added to the structure affected the pain perception of mice.

This study consisted in a modified tail-flick (used to test efficacy of a drug) where the mice were subjected, and their tails submerged in a 55ºC water bath. Previously to that, the mice were administered with different synthesized β-endorphins that differed in presence of a glucose, a lactose, or not any carbohydrate in the structure. As β-endorphin is known for its antinociceptive properties the period of time between dipping the mice tails into the warm water until the moment they flexed their tail in response of the heat was measured, with an error of 0,1s. This experiment would show if this glycosylated peptide would cross the blood-brain barrier more easily, reaching the brain and decreasing even more the detection of the painful stimulus [29].

Table 4 and 5. Calculated potency of the administered β-endorphin analogues, R being the carbon moiety of the peptide. The tables correspond to the values obtained by i.c.v (intracerebroventricular) and i.v (intravenous) administration respectively [29].

Linker Address		A_{50} Values, nmol (95% Confidence Intervals)		
		R = OLact	R = OGlc	R = OH
Helicity (Low → High)	BB	0.63 (0.51-0.78)	1.27 (0.59-2.9)	1.89 (1.4-2.7)
	BA	0.25 (0.19-0.32)	0.68 (0.50-0.92)	0.18 (0.14-0.25)
	AB	0.84 (0.71-0.98)	1.61 (0.8-3.0)	0.55 (0.32-0.95)
	AA	0.24 (0.19-0.31)	1.66 (0.93-2.9)	0.66 (0.50-0.87)
	AG	0.16 (0.15-0.17)	1.66 (1.0-2.8)	0.90 (0.64-1.3)
	GA	0.59 (0.44-0.81)	2.87 (1.5-5.5)	1.10 (0.50-2.4)
	GG	0.26 (0.21-0.33)	2.39 (1.7-3.4)	2.19 (1.6-3.0)

Linker Address		A_{50} Values, μmol/Kg (95% Confidence Intervals)		
		R = OLact	R = OGlc	R = OH
Helicity (Low → High)	BB	3.89 (3.0-5.1)	3.39 (2.6-4.5)	>14.9 (n/a)
	BA	0.96 (0.67-1.4)	0.32 (0.24-4.2)	>4.72 (n/a)
	AB	1.11 (0.93-1.33)	3.86 (3.0-5.0)	>4.75 (n/a)
	AA	3.71 (2.6-5.3)	4.30 (3.3-5.7)	>4.75 (n/a)
	AG	7.91 (5.3-11.8)	4.07 (2.9-5.8)	>4.78 (n/a)
	GA	1.19 (0.88-1.6)	3.43 (2.6-4.5)	>4.78 (n/a)
	GG	>4.16 (n/a)	4.21 (3.0-5.9)	>4.81 (n/a)

Both tables display their results in A_{50}. A_{50} (also EC_{50} or Half maximal effective concentration) is the magnitude that measures the concentration of a drug or toxin needed to obtain half of the maximum response after an exposure time, so

a drug is more effective if the value is little, as less concentration is needed to obtain results [30].

As seen in Table 4, all the tested peptides (the one with a glucose, the one with a lactose and the one without carbohydrate) showed positive results when injected directly through the brain. On the other hand, when the different substances are intravenously administered (Table 5), it can be seen that both glycopeptides have far lower A_{50} values than the ones of the non-glycosylated β-endorphin, which compared to Table 4 have increased greatly. This showed that the non-glycosylated compound had very poor BBB penetration compared to the glycosylated compounds, which could cross the BBB and reach the CNS, having a much greater antinociceptive effect on the mice.

The results of this study concluded that the presence of a carbon moiety increased BBB penetration, proving glycosylation to be a successful method to improve drug transport to the central nervous system [29]. Other studies, like the use of glycosylation to improve the transport and potency of DAMGO [31] also endorse this statement.

3.5. SOLID PHASE PEPTIDE SYNTHESIS

The synthesis of the glycopeptide of $PACAP_{23}$ is achieved through solid phase peptide synthesis (SPPS) by the incorporation of a glycosylated amino acid, and then the addition of the different amino acids of the chain.

Solid-phase synthesis is one of the most used methods for the synthesis of peptides. Even though peptides are biologically synthesized from the N-terminal (amino group side), this is not the case in Solid-phase peptide synthesis, in which the synthesis is carried out from the C-terminal to the N-terminal (carbonyl group side). The most used protecting groups are Fmoc (9-fluorenylmethyloxycarbonyl group) and Boc (tert-butoxycarbonyl).

For this synthesis, the carboxyl group of the first amino acid binds to a deprotected solid material or resin (usually low cross-linked polystyrene beads), forming ester or amide bonds. Once the first amino acid is bonded to the linker, to avoid for the next amino acids to bind to some spaces that could have remained unreacted during the reaction with the first amino acid, a capping step is carried out. After the remaining positions have been linked, the amino group of the bound amino acid is deprotected and reacts with the Fmoc protected amino acid, forming a dipeptide. This reaction consists in a nucleophilic attack of the N-terminal of the last amino acid added to the carboxylic groups of the added one.

This cycle continues until the last amino acid is added to the peptide chain, and then the peptide is separated from the resin beads using a cleavage cocktail. To ease the linking of the peptides and to prevent an acid-base side reaction

between the amino acids, a coupling reagent is used. The function of this coupling reagent is to activate the carboxylic group of the entering amino acid by increasing the leaving group capacity of the hydroxyl.

It is also important to take into consideration that some amino acids contain functional groups that need to be protected prior the synthesis to avoid any undesirable side reactions [32].

Before beginning the SPPS process is very important to select the most suitable solid resin to carry out the synthesis. This resin is a polymeric support bonded to a linker, which is the compounds that binds to the first amino acid to begin the synthesis of the peptide chain. Usually, the polymer forming the resin is 1-2 % cross-linked poly(styrene-divinylbenzene), and there are different bead sizes: from 75 to 150 microns, and from 35 to 75 microns of diameter.

One of the most important properties for the resin is its swelling factor. Swelling is a critical step in the synthesis due to the fact that the peptide synthesis is performed in the swollen network of the resin. As you can see in Figure 8, the sites available for the first amino acid to link to depend in the swelling of this polymeric solid support, meaning that the kinetics of the SPPS reactions depend on the diffusion rate of the reactants and reagents in this network. This causes that a resin capable of more swelling could be more favorable for Solid-phase peptide synthesis, as it would increase the diffusion rate, meaning higher reaction velocity and usually better chemical conversions.

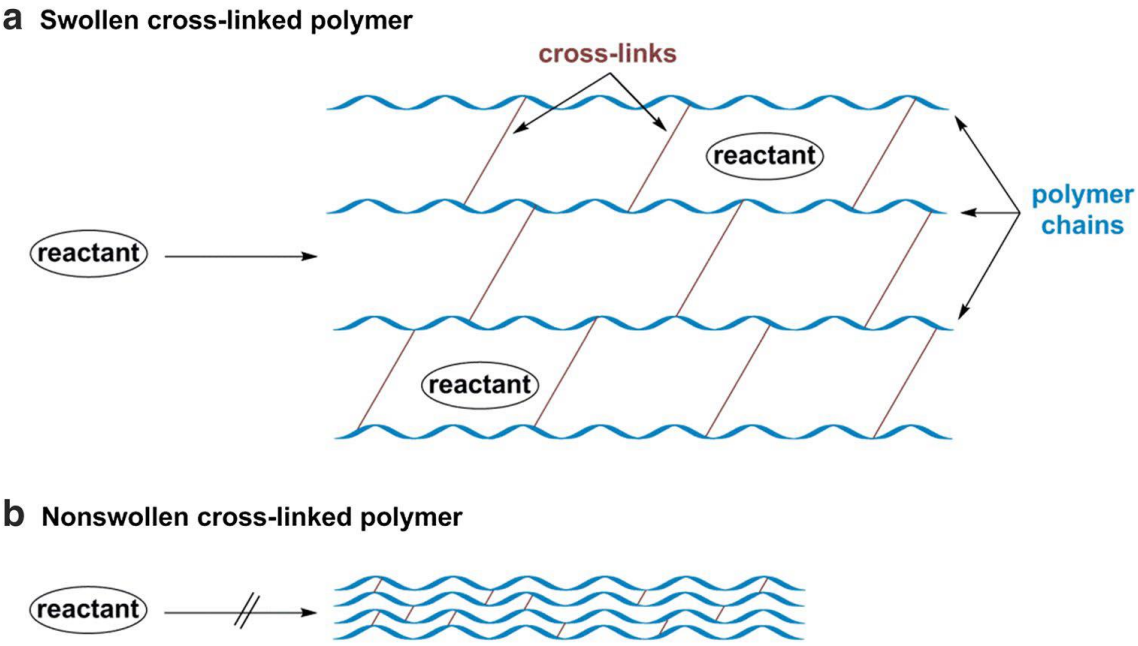

Figure 8. Swelling effect of a solvent in the polymer solid resin [32].

This swelling is caused by the occupation of the space between the resin polymer chains by the solvent molecules, expanding the resin and increasing the probability for the reagents to reach the free positions and react. This property is reduced if the polymer has a higher degree of crosslinking, decreasing the

diffusion rate of the reagents and hindering the reaction. In this case, in order to increase the swelling of these kinds of resin, aprotic solvents like DCM are used.

Now focusing about the linkers, there are some factors that must be taken into account in order to choose the perfect linker. Since linkers are key to the correct binding and cleavage of the peptide, a suitable linker must be able to immobilize the first amino acid with high yield. It also needs to remain stable and unreacted with all the reactants, solvents and cocktails used during the chain synthesis. Finally, it must be easy for the finished peptide chain to be cleaved from the linker avoiding the formation of any side product [33].

Another important topic to discuss is the proportion of the first peptide to use in comparison to the amount of available positions in the resin. Although it would be logical to use a similar proportion or even higher to ensure the occupation of the maximum number of available spaces, it has been studied that the elevated concentration of the amino acid can cause an increase in the appearing of undesired side-reaction during the binding.

Side-reactions can happen during all the steps of the synthesis. The most common ones are aspartamide formation, methionine oxidation, and trifluoroacetylation. Most of these reactions can be avoided with the correct selection of resin, linkers, and being careful of the functional groups of the peptide chain (usually by using protected amino acids to avoid any problem) [32].

4. EXPERIMENTAL PART

The experimental part of this bachelor's thesis consists in the synthesis of four glycosylated $PACAP_{23}$ compounds by solid-phase peptide synthesis. SPPS allows the synthesis of long peptide chains in a reduced time compared to other synthetic methods. During this process, several HPLC analysis were performed to check the correct development of the synthesis and the presence of any side products. As said in the summary of the Bachelor's Thesis, the experimental part was entirely developed in Dr. Robin Polt's research group at The University of Arizona.

As can be seen in Table 6, the compounds only differ in the carbon moiety of the structure. In all the designed peptides the carbohydrate part will be different. These compounds will be latter studied both *in vitro* and *in vivo* the measure how the stability and the blood-brain barrier penetration vary with different carbon moieties. From these values, it will be extracted which of the carbohydrates is more effective to improve the properties of $PACAP_{23}$.

Table 6. Partial structure and names of the designed $PACAP_{23}$ compounds.

Compound Name	Structures
CRA_DV_3022	$XXXXXXXXXX_{10}XXXXXXXXXK_{20}KYL\text{-}CM_1\text{-}CONH_2$
CRA_DV_3023	$XXXXXXXXXX_{10}XXXXXXXXXK_{20}KYL\text{-}CM_2\text{-}CONH_2$
CRA_DV_3024	$XXXXXXXXXX_{10}XXXXXXXXXK_{20}KYL\text{-}CM_3\text{-}CONH_2$
CRA_TG_3025	$XXXXXXXXXX_{10}XXXXXXXXXK_{20}KYL\text{-}CM_4\text{-}CONH_2$

4.1. SYNTHESIS OF THE GLYCOSILATED AMINO ACIDS

Before the synthesis of the peptide chain, it is necessary to synthesize the glycosylated amino acids that will be used in the future peptide chain. From these selected amino acids, Fmoc protected serine glucoside and lactoside were produced in the laboratory.

4.1.1. Synthesis of Fmoc-Ser(Glc(OAc)$_4$)-OH

It was the first reaction performed. Until some years ago, the most used method to carry out the synthesis of this compound consisted in more than ten reactive steps which led to little yields, sometimes of even less than 1%. Since then, research on this topic has been able to provide a direct method consisting in a one-step reaction with a later treatment procedure to isolate and purify the serine glucoside. The method used in the laboratory was proposed by one of the members of the research group that had improved and simplified the isolation steps.

Glycosylation of N-Fmoc-Serine-OH with β-Peracetyl Glucose

This reaction involves the reaction of β-Peracetyl Glucose[34] and N-Fmoc-Ser-OH[35] in $CHCl_3$ and with $InBr_3$ acting as a catalyst of the reaction.

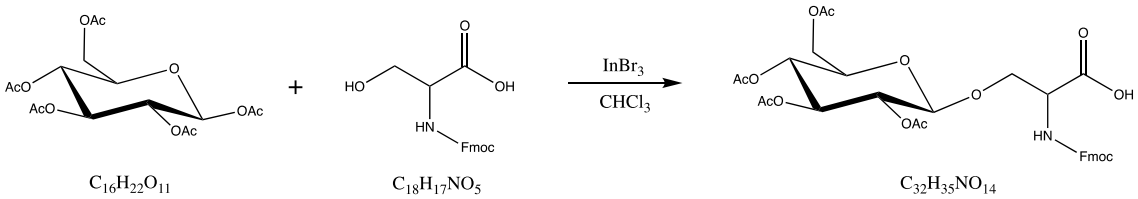

Figure 9. Reaction scheme for the glycosylation of N-Fmoc-Serine-OH with β-Peracetyl Glucose.

First of all, 1 equivalent of N-Fmoc-Ser-OH is put into reflux with 3 equivalents of β-glucose and a catalytic amount of $InBr_3$ (0.25 eq.), and chloroform. The reflux was left overnight at 85ºC and an HPLC was done to check the conversion of the reaction. Once the reaction was finished, the solvent was evaporated and co-evaporated with ethyl acetate three times in a rotavapor.

After that, the slurry brown solid obtained was dissolved in EtOAc and, to remove any residual $InBr_3$, the solution washed with deionized water three times in a separation funnel. Then, the organic layer was washed with $NaHCO_3$ and then extracted with water. The water phase obtained was analyzed with an HPLC and the process was repeated until there was no significant amount of our desired compound left in the organic phase (also determined using HPLC).

Following this, the water phases were combined and acidified until pH 2 by adding 1 M HCl solution dropwise while stirring the combined phases using a stirring plate. The brown oil that crashed out as a consequence of the acidification was extracted with EtOAc three times, and the phases were combined and dried using $MgSO_4$.

The next step was to evaporate and co-evaporate the solution with MeOH three times. The clear brown solid obtained was recrystallized with MeOH using a heat gun (MeOH is a suitable solvent for recrystallization because the product is fairly insoluble in MeOH at room temperature, but it can be dissolved when heating the mixture). The hot solution was placed in an Erlenmeyer with seed crystals and left overnight.

Finally, the white solid that recrystallized was filtered using a Buchner funnel and cold MeOH, and the mother liquor is analyzed by HPLC to check if there is still some of our product. In affirmative case, the mother liquor is evaporated in a rotavapor and the recrystallization process was repeated until the measured mother liquor indicates that almost all the product had been recovered.

The characterization of the compounds was performed by using both HPLC and H^1 NMR analysis, which will be discussed in detail in the Results and Discussion section.

4.1.2. Synthesis of Fmoc-Ser(Lac(OAc)$_7$)-OH

Lactose needs more favorable conditions to carry out the glycosylation reaction the same way as in the case of glucose. Because of that, it was used Fmoc-Ser(OBn) instead of Fmoc-Ser-OH, which was synthesized previous to this procedure.

Glycosylation of Fmoc-Ser(OBn) with β-Peracetyl Lactose

First, 1 equivalent of Fmoc-Ser(OBn)[36] and 1.25 equivalents of β-Peracetyl Lactose[37] were weighted and added to a round bottom flask, and then dissolved with CCl_4. The reagents were put into reflux at 90ºC, and after 2 hours, 0.1 equivalents of $InBr_3$ were added to favor the reaction.

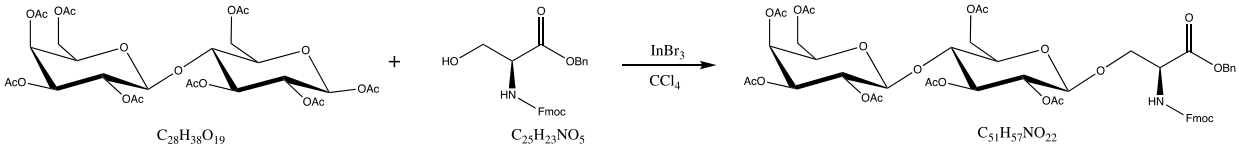

Figure 10. Synthetic scheme for the Glycosylation of Fmoc-Ser(OBn) with β-Peracetyl Lactose.

The progress of the reaction was monitored using HPLC measurements until the conversion was high enough to stop the reflux and continue with the procedure.

After that, the resulting solution was evaporated and co-evaporated first three times with EtOAc, and then three more times with Et_2O to remove the CCl_4 from the reaction. The solid was then dissolved in EtOAc and washed with water and a brine in a separation funnel. The yellow organic phase was then dried, evaporated and co-evaporated with DCM and finally the white solid was dissolved in DCM.

The next step was to separate our desired compound from any residual unreacted reagents with a Biotage auto-column separation. To do this, the first step was to choose the suitable mobile phase for the separation. To do this, several TLCs were done, resulting in the election of 6:4 Hexanes/EtOAc as the mobile phase for the separation. Another advantage of this mobile phase was that our desired product was the last to come out from the column, easing the separation process.

During the auto-column process, the liquid coming out of the column was being collected in different Erlenmeyers. At the same time, TLCs were performed to identify when the desired compound was going to come out.

When the TLC gave a positive result (the Fmoc-Ser-Lactose was the only compound that was both visible both in UV and by H_2SO_4 stains), the solution

coming out was collected for it to be finally evaporated and co-evaporated with Et_2O, obtaining our isolated compound of interest.

The characterization of the compounds was performed by using an HPLC, which will be discussed in detail in the Results and Discussion section. An H^1 NMR spectrum was not necessary this time for recommendation of the research group.

4.2. SYNTHESIS OF THE PEPTIDE CHAIN BY SPPS

The synthesis of the glycosylated compounds was carried out on a Prelude® automated peptide synthesizer (Figure 11). The process was developed both in automated and semi-automated modalities, in which the reactants were added with a syringe directly into the rection vessel. It is important to remark that for the entire duration of the synthesis procedure, the reaction vessel with the resin is mixed with argon from the bottom of the device, and each and all of the washings performed before and after the different steps of the procedure were done with DCM and DMF for 2 minutes.

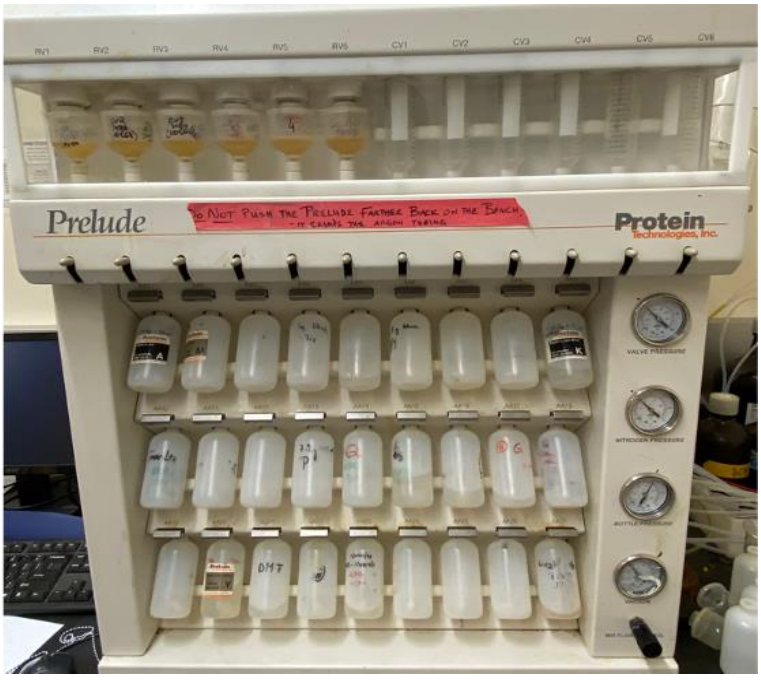

Figure 11. Prelude® automated peptide synthesizer used by the Polt's group.

Preparation of the resin

The resin used in the synthesis procedure was a Rink Amide-MBHA resin (Figure 12). 0.6g of this resin (0.25 mmol) were weighted and deposited in 45 ml reaction vessel, where it was placed to swell during 1 hour in DMF. The removal of the Fmoc protecting group was performed by adding a 2% DBU and 2%piperidine in DMF (total of 6mL) solution and mixing it for 4 minutes. After draining the vessel, the resin was washed with 6 ml of DMF. After that, the removing process was repeated during 8 minutes with 6 additional DMF washes.

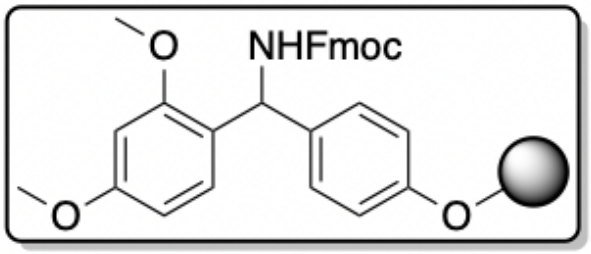

Figure 12. Structure of the Rink Amide-MBHA resin used in the SPPS process.

Loading of the first amino acid to the resin

As the designed compounds contain different carbohydrate moieties, 0.8 equivalents of the first amino acid (0.2 mmol) were used in in each case. All the individual amino acid was placed with 0.8 equivalents 6-Cl-HOBt in a vial, and the mixture was dissolved with 4 ml of NMP (N-Methyl-2-pyrrolidone). After that, 0.8 equivalents of DIC were added to the vial. To ensure that everything was dissolved, the vials were sonicated and vortexed for 1 minute, and then the vials were poured into their respective reaction vessels, leaving them to mix for 16 hours. Later, 10 ml of DMF were added and drained immediately, followed by 6 washings with 6 ml of DMF and 6 more washings with 6 ml of DCM.

After the reaction was completed, the resin NH_2 sites than remained unreacted were capped using a solution consisting in 10% N,N-diisopropylethylamine and 10% Ac_2O in 8mL of DCM. This reaction was left for 1 hour, and then the resin was washed 6 times with DCM and 4 times with DMF, preparing the resin for the next reactive steps.

Loading of Additional amino acid in CRA_DV3024

An additional synthetic step had to be performed for the synthesis of CRA_DV_3024. To do so, 2 equivalents (0.5 mmol) of the selected amino acid and 2 equivalents (0.5 mmol) of 6-Cl-HOBt were placed into a vial and dissolved in 4 ml of NMP. Then, 2 eq. DIC was added to the vial and the mixture was sonicated and vortexed for 1 minute to ensure everything is dissolved. After that, the solution was added to the reaction vessel and the reaction was left mixing for 16 hours. Following that, 10 ml of DMF were added to the vessel, draining it immediately. Finally, the resin was washed with 6 ml of DMF 6 times.

First Prelude® automated synthesis step

The amino acids from Leu^{23} to X^{10} in the peptide chain were added by automatic SPPS mode on the Prelude® automated peptide synthesizer using the same procedure. The Fmoc group of the first amino acids was removed using the deprotection solution described before. Then, 2 eq. of the desired amino acid together with 2 eq. of HBTU and 10 eq. of *N*-methylmorpholine were added in a special container of the Prelude®, and poured into the reaction vessel with the resin. The reaction vessel was mixed for 30 minutes and then the resin was

washed with 6 ml of DMF. The mixing was repeated for 30 more minutes to guarantee the success of the coupling, and the vessel was washed 6 times with DMF. The deprotection and coupling steps explained were repeated up to the coupling of X^{10}.

Manual loading of XX dipeptide

The addition of a dipeptide instead of the individual amino acids is explained due to the presence of some specific amino acids, which, due to exposure to basic conditions during the synthesis process, can lead to aspartimide formation (Figure 13), a common phenomenon in peptide synthesis with the capacity of forming a number of different side products, decreasing the purity of the final peptide [38].

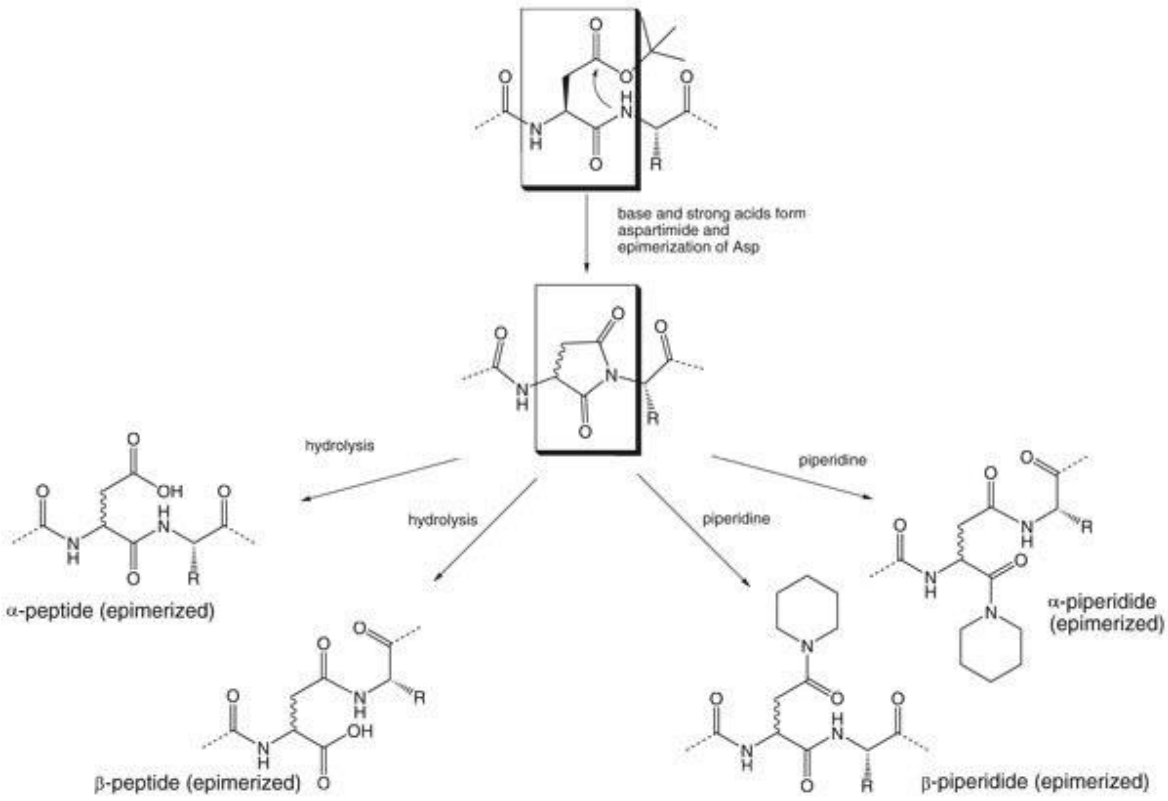

Figure 13. Aspartimide formation process with the formation of some side products [38].

For this dipeptide coupling, the Fmoc group from the X^{10} is first deprotected following the usual procedure. Secondly, 1.2 equivalents of Fmoc-XX-OH (0.3 mmol) and 1.2 equivalents of 6-Cl-HOBt (0.3 mmol) were added to a vial for each peptide. Then, 4 ml of NMP and 1.2 equivalents of DIC (0.3 mmol) were added to the mixture. The vial was sonicated and vortexed for 1 minute, and then the vials were added to the reaction vessels. The vessels were mixed with argon overnight for 16 hours. After that, the mixture of the reaction vessels was dilute with 10 ml of DMF and then drained. Finally, the resin was washed with 6 ml of DMF 6 times.

Second Prelude® automated synthesis step

The amino acids of the chain from X^5 to X^7 were added by automatic SPPS mode on the Prelude® automated peptide synthesizer using the same procedure. The Fmoc group of the last amino acid added was removed using the usual deprotection solution. Then, 4 equivalents of the desired amino acid, together with 4 eq. of HBTU and 16 eq. of *N*-methylmorpholine, all in 10 ml of DMF, were added in a special container of the Prelude®, and then poured into the resin. The vessel was mixed for 30 minutes, and then the resin was washed once with DMF (6 ml). The mixing was repeated for 30 more minutes to guarantee the success of the coupling, and the vessel was washed 6 times with DMF. The deprotection and coupling process explained was repeated up to X^5.

Manual loading of XX dipeptide

For this second dipeptide coupling, the Fmoc group from the X^5 is first deprotected following the usual procedure. Secondly, 2 equivalents of Fmoc-XX-OH (0.5 mmol) and 2 equivalents of 6-Cl-HOBt (0.5 mmol) were added to a vial for each peptide. Then, 4 ml of NMP and 2 equivalents of DIC (0.5 mmol) were added to the mixture. The vial was sonicated and vortexed for 1 minute to ensure solubilization, and then the vials were added to the resin. The reaction mixture was mixed with argon for 16 hours. After that, the mixture was diluted with 10 ml of DMF and immediately drained. Finally, the resin was washed 6 times with 6 ml of DMF.

Manual loading of the remaining amino acids: Fmoc-X^2(tBu)-OH and Fmoc-X^1(Trt)-OH

For the coupling of the last two amino acids, the Fmoc protecting group of the last amino acid was first deprotected as explained before. Secondly, 4 equivalents of the amino acid in question (1.0 mmol), and 4 equivalents of 6-Cl-HOBt (1.0 mmol) were mixed in a vial. Then, the mixture was dissolved in 4 ml of NMP, and 4 equivalents of DIC (1.0 mmol) were added. The reagents were sonicated and vortexed for 1 minute and poured into the reaction vessel. The vessel was left stirring for 1 hour. Afterwards, 10 ml of DMF were added to the resin and then the vessel was drained. After the resin was drained, it was washed 6 times with 6 ml of DMF. Finally, the X^1 was deprotected using the usual procedure.

Cleavage of the acetyl groups

In order to get rid of the acetyl groups of the carbohydrates contained in the peptide structure, a 120 ml solution consisting in 50% NH_2NH_2 x H_2O in NMP was prepared, and 10 ml were poured in each of the reaction vessels. Then, the vessels were left mixing for 16 hours. After that, the resin was drained, and an additional 10 ml of the prepared solution was added to each reaction vessel. The resins were left mixing for another 2 hours and then the resin was drained from the 50% NH_2NH_2 x H_2O. Afterwards, the resin was washed 8 times with 10 ml of

DMF, 8 times with 10 ml of DCM, and finally the resin was dried under vacuum for three hours.

Cleavage from the resin and global side chain deprotection

To separate the peptide chain from the linker, the resin was dried, and a cleavage cocktail was added to the reaction vessel, leaving the resin mixing for 60 minutes. This cocktail contained TFA, DCM, H_2O, triethylsilane, and anisole with a proportion of 90:10:2:3:0.5. After mixing the resin, the solution was collected into a 45 ml centrifuge tube. To make sure that most of the separated peptide was collected, the cleavage process was repeated 2 times for periods of 10 minutes each.

After these cleavage steps, the combined fractions obtained were evaporated with argon until the peptide began to crash out. Following that, about 40 ml of ether were added to each tube to aide in the precipitation of the peptide chain. The tubes were then centrifuged for 10 minutes at 5 G. This ether layer was then removed by decantation and the centrifuge and decantation process was repeated two more times. Once the last decantation was performed, the crude peptides obtained from each tube were left to dry overnight.

4.3. PURIFICATION OF THE $PACAP_{23}$ GLYCOPEPTIDES

Once the synthesis of the peptides was complete, the crude compounds were purified making use of a Gilson system with a UV detector (at 280 nm). The column used was a Vydak C18 preparative reversed-phase column (250 mm x 50 mm), and the gradient selected for the process was 5-80% CH_3CN vs 0.1% CF_3COOH in H_2O over 60 min, all this to be able to obtain the glycopeptides in pure form.

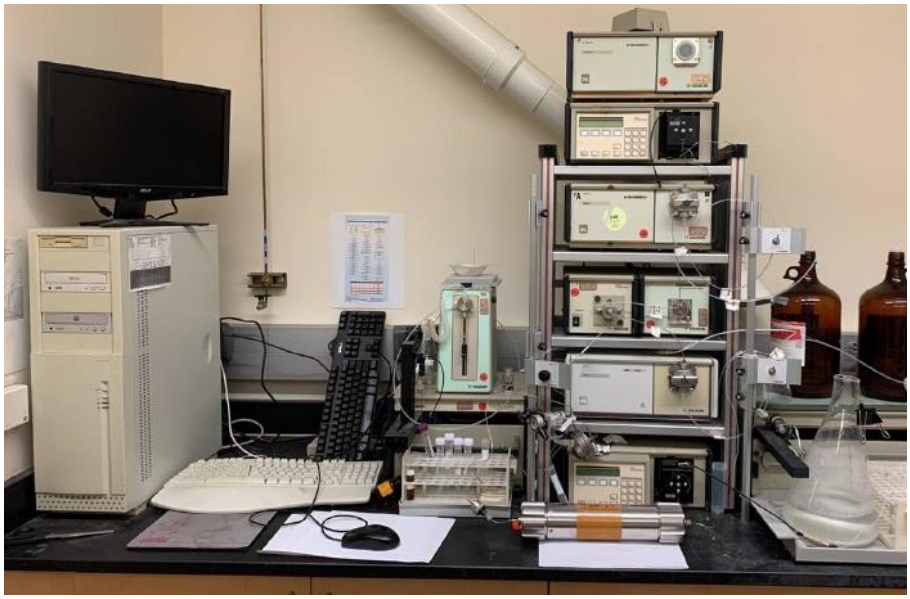

Figure 14. Set up for the preparative HPLC.

The pure glycopeptide fractions obtained from the preparative HPLC were frozen at -80ºC, to be later lyophilized to acquire the synthesized compounds as white and soft solid.

The purity of the compounds was assessed by HPLC analysis, using an Inspire C18 5µm 250 mm x 4.6 mm column, with a Varian LC with a diode array detector system (at 280 nm). The gradient employed in the analysis was the same as the one used in the purification over a span of 15 minutes. The pure glycopeptides were finally characterized by mass spectrometry (ESI-MS).

5. RESULTS AND DISCUSSION

5.1. CHARACTERIZATION AND PURITY OF Fmoc-Ser(Glc(OAc)$_4$)-OH

Three different batches of the compound were prepared (Table 7), in which the amount of starting materials was increased: a batch beginning with 10g Fmoc-Ser-OH (the limiting reagent of the reaction), a 20g batch, and a 25g one.

Table 7. Amounts, yields and purity of the Fmoc-Ser-Glucose batches.

	10g batch	***20g batch***	***25g batch***
Theoretical yield (g)	20.07	40.15	50.17
Amount Obtained (g)	6.09	12.00	17.54
Yield (%)	30	30	35
Purity (%)	97.94	97.22	97.31

As explained in the experimental part, all the batches were characterized using HPLC and H^1NMR. First talking about the HPLC, after checking the purity of all the batches, all of them were in the range of 97-98%, which was a higher value than the one expected, especially in the case of the first batch (Figure 15), which had the best purity value although it was the first time performing the reaction.

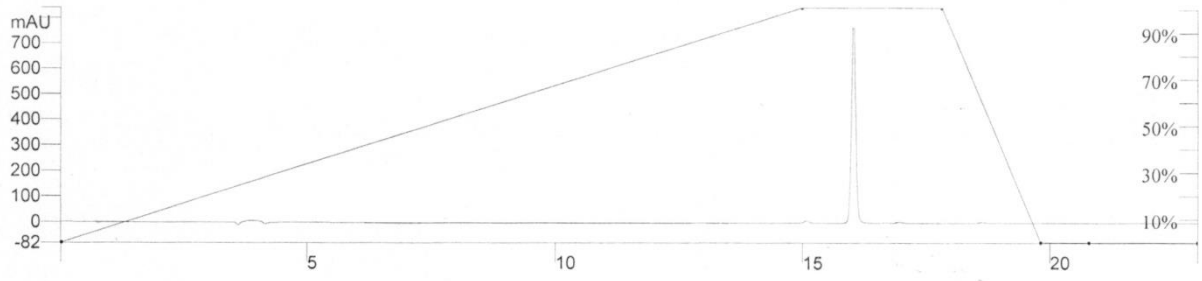

Peak No	Peak Name	Result ()	Ret. Time (min)	Time Offset (min)	Area (counts)	Rel Ret Time	Sep. Code	Width 1/2 (sec)	Status Codes	Group
1		1.1334	15.088	0.000	281314	0.00	BB	5.6		0
2		97.9440	16.029	0.000	24310676	0.00	BB	5.8		0
3		0.5043	16.947	0.000	125171	0.00	BB	5.1		0
4		0.4183	18.621	0.000	103826	0.00	BB	5.3		0
	Totals	100.0000		0.000	24820986					

Figure 15. HPLC of the first batch of Fmoc-Ser(Glc(OAc)4)-OH.

In the case of the H^1NMR, the measured spectrum was compared with the theoretical spectrum for the Fmoc-Ser(Glc(OAc)4)-OH, concluding that they were very similar and the product was pure (Figure 16).

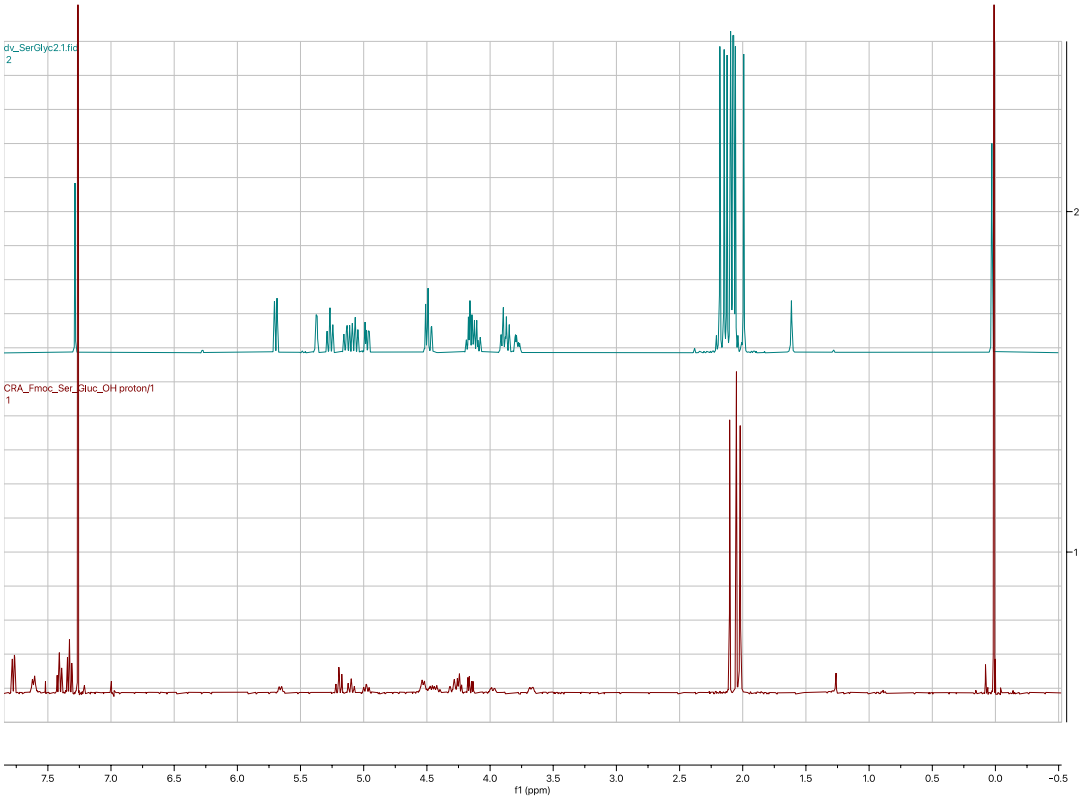

Figure 16. H^1NMR spectrum of the produced Fmoc-Ser(Glc(OAc)4)-OH (green) compared to the one provided by the research group (red).

In conclusion, even though the yield of the reaction was relatively low, it entered in the levels expected. Regarding the purity of the compound, it was considerably high, resolving in the success of the synthesis.

5.2. CHARACTERIZATION AND PURITY OF Fmoc-Ser(Lac(OAc)$_7$)-OH

Looking at Table 8, two batches of Fmoc-Ser(Lac(OAc)7)-OH were prepared, one starting with 5g of Fmoc-Ser(OBn) and another one starting with 15g.

Table 8. Amounts, yields and purity of the Fmoc-Ser(Lac(OAc)7)-OH batches.

	5g batch	***15g batch***
Theoretical yield (g)	6.2	18.60
Amount Obtained (g)	3.27	13.14
Yield (%)	53	71
Purity (%)	84.06	87.05

As discussed in the experimental part of the Bachelor's Thesis, to check the purity of the synthesized compound, an HPLC analysis was performed (Figure 17).

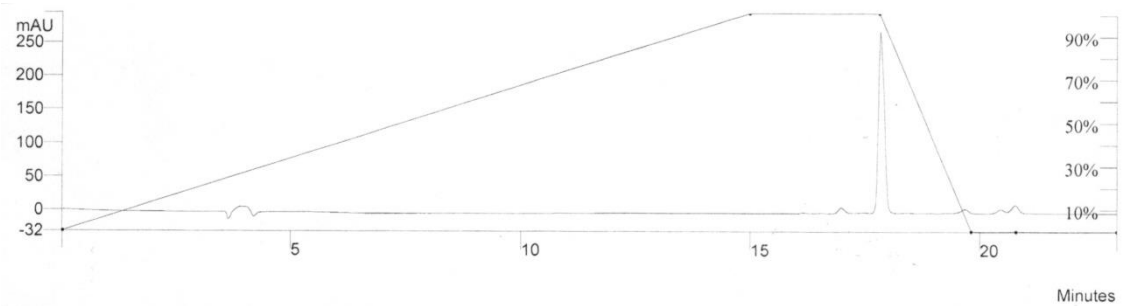

Peak No	Peak Name	Result ()	Ret. Time (min)	Time Offset (min)	Area (counts)	Rel Ret Time	Sep. Code	Width 1/2 (sec)	Status Codes	Group
1		2.7872	16.979	0.000	400684	0.00	BP	8.8		0
2		0.3757	17.448	0.000	54016	0.00	TS	0.0		0
3		87.0498	17.851	0.000	12514066	0.00	PB	8.8		0
4		2.4871	19.672	0.000	357540	0.00	BP	10.2		0
5		2.2840	20.461	0.000	328342	0.00	PV	10.7		0
6		5.0161	20.776	0.000	721104	0.00	VB	10.4		0
	Totals	99.9999		0.000	14375752					

Figure 17. HPLC of the synthetized Fmoc-Ser(Lac(OAc)7)-OH.

From this analytical method, it was concluded that although the purity of the compound was lower than in the case of the Fmoc-Ser(Glc(OAc)4)-OH, it was expected, because from the research group it was indicated that the complexity of the reaction and the isolation steps could reduce the purity of the product.

5.3. CHARACTERIZATION AND PURITY OF PACAP$_{23}$ GLYCOPEPTIDES

As explained before, the purity of the glycopeptides was assessed a HPLC analysis for each of the compounds. After that, mass spectrometry was performed to the glycopeptides to make sure the peptide synthesized was the correct one.

5.3.1. EVALUATION OF THE PURITY BY HPLC

CRA_DV_3022

As can be seen in Figure 18, the purification method carried out by the preparative HPLC achieved to obtain the mostly pure peptide, with a 100% purity of the sample. Looking at the graphic, the peak displayed is narrow, with a little shoulder on the left.

CRA_DV_3023

Looking at Figure 19, the purity of the sample was of 100%, with the peak displayed in the graphic presenting a shoulder to the left and a shoulder to the right.

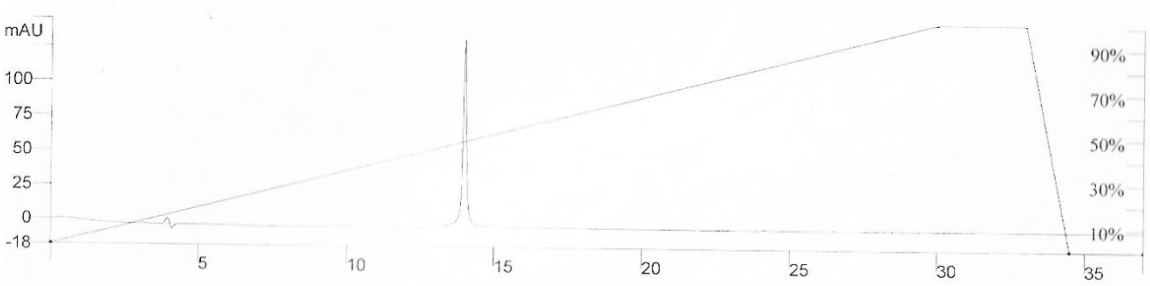

Peak No	Peak Name	Result ()	Ret. Time (min)	Time Offset (min)	Area (counts)	Rel Ret Time	Sep. Code	Width 1/2 (sec)	Status Codes	Group
1		100.0000	13.984	0.000	6515282	0.00	BB	7.0		0
	Totals	100.0000		0.000	6515282					

Figure 18. HPLC of the purified CRA_DV_3022.

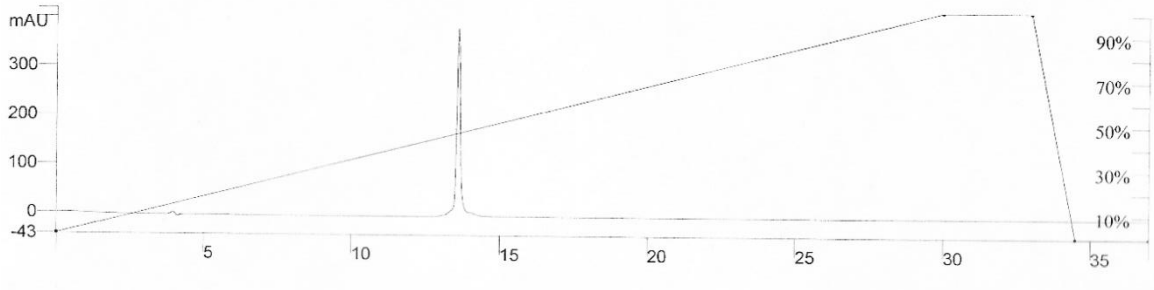

Peak No	Peak Name	Result ()	Ret. Time (min)	Time Offset (min)	Area (counts)	Rel Ret Time	Sep. Code	Width 1/2 (sec)	Status Codes	Group
1		100.0000	13.595	0.000	18338214	0.00	BB	7.2		0
	Totals	100.0000		0.000	18338214					

Figure 19. HPLC of the purified CRA_DV_3023.

CRA_DV_3024

Focusing on CRA_DV_3024, the sample analyzed by HPLC showed a 100% purity. As showed in Figure 20, in the graphic appears a single narrow peak with a shoulder on the left.

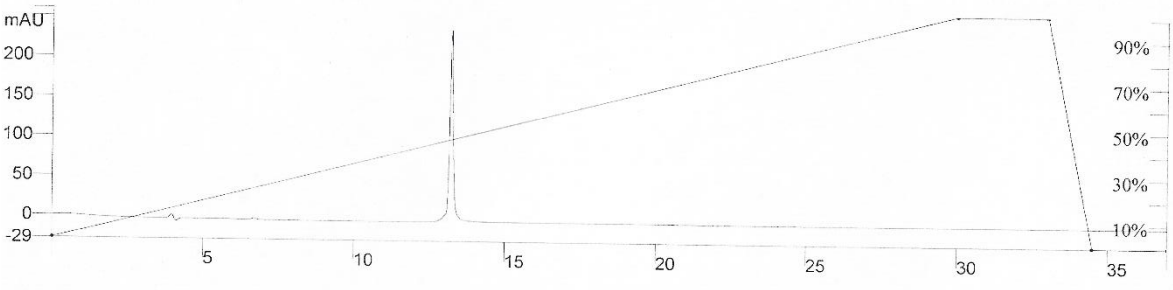

Peak No	Peak Name	Result ()	Ret. Time (min)	Time Offset (min)	Area (counts)	Rel Ret Time	Sep. Code	Width 1/2 (sec)	Status Codes	Group
1		100.0000	13.235	0.000	10758523	0.00	BB	7.0		0
	Totals	100.0000		0.000	10758523					

Figure 20. HPLC of the purified CRA_DV_3024.

CRA_TG_3025

As can be seen in Figure 21, the CRA_DV_TG_3025 sample showed a purity of 100%. Looking at the graphic, the peak displayed presents tailing to the left, and a shoulder on the right.

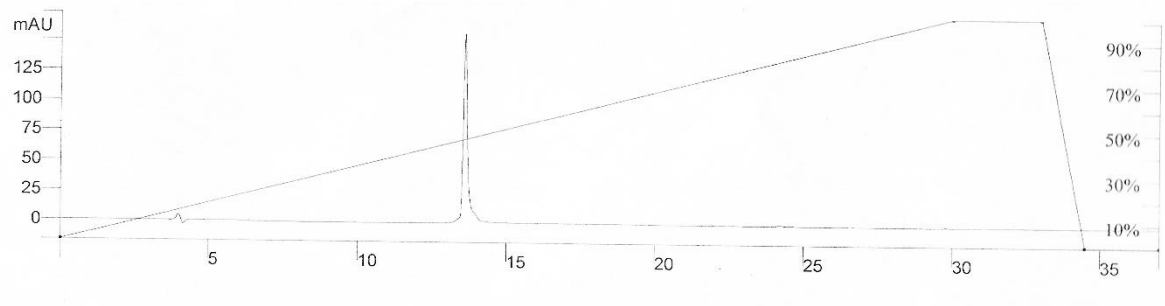

Peak No	Peak Name	Result ()	Ret. Time (min)	Time Offset (min)	Area (counts)	Rel Ret Time	Sep. Code	Width 1/2 (sec)	Status Codes	Group
1		100.0000	13.587	0.000	8293504	0.00	BB	7.8		0
	Totals	100.0000		0.000	8293504					

Figure 21. HPLC of the purified CRA_TG_3025.

5.3.2. YIELD OF THE SYNTHESIZED COMPOUNDS

Once the compounds were recovered and stored, the yield of the synthesis was calculated. It is important to mention that the yield values were provided by the research group, but the method of calculation was not issued. From these results, it can be concluded that the synthesis was a success because the after the synthesis and the purification of the peptides, it was obtained enough amount of all of the compounds proceed with the characterization and the *in vitro* and *in vivo* studies.

Table 9. Yield of the produced glycopeptides.

COMPOUND	***YIELD (mg)***
CRA_DV_3022	18.1
CRA_DV_3023	23.5
CRA_DV_3024	7.7
CRA_TG_3025	36.0

5.3.3. CHARACTERIZATION OF THE PACAP$_{23}$ GLYCOPEPTIDES

Once the analysis by HPLC showed that the compounds synthesized and purified were pure, a sample of each compound was sent to carry out an electrospray ionization mass spectrometry (ESI-MS), in order to confirm the identity of the compounds. Electrospray ionization method is used especially the case of proteins, synthetic polymers or carbohydrates.

An important fact about electrospray ionization is that aside from the formation of single charged molecules, it is also possible to produce compounds with multiple

charges in the presence of bigger compounds. This fact is positive because it allows the mass spectrometer to measure the spectrum of more massive compounds despite having a relatively limited range, also easing molecular weight calculations. The multiple charge molecules phenomenon happens in the case of bigger molecules like peptides, where it is common to find more than one basic residues, allowing for more protons to bind to these basic sites, increasing the charge of the fragment [39].

As can be seen in Figure 22, the mass of each multiply charged compound consists in adding the number of protons bonded to the compound during the process to the total molecular weight and dividing it by this same number of positive charges. The process of characterization consisted in the comparison between the calculated molecular mass of the compounds with the measured molecular mass from the samples' spectra.

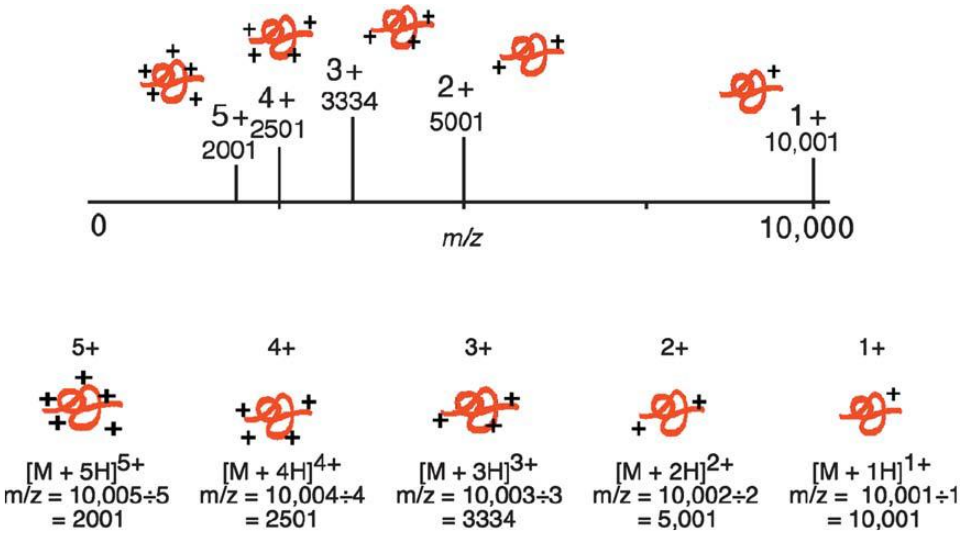

Figure 22. Representation of an ESI-MS spectrum with multiply charged molecules [39].

CRA_DV_3022

The mass spectrum for CRA_DV_3022 can be seen in Figure 23, where appear fragments from 3+ to 6+. As an example for the calculation of the measured molecular weight in multiply charged molecules, the molecular weight for the 4+ charged molecule is 712.95 g/mol. This number multiplied by 4 gives 2851.8, and then 4 is subtracted, resulting in a molecular weight of 2847.80 for the compound.

Looking at Table 10, the results of the measured molecular weight are very similar to the exact mass calculated for the peptide, concluding that the synthesized compound corresponds to the theorized one.

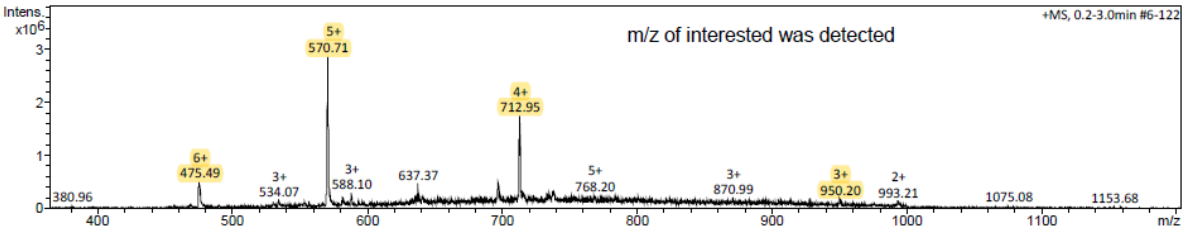

Figure 23. ESI-MS spectrum for CRA_DV_3022.

Table 10. Comparison between the calculated molecular weight of CRA_DV_3022 with the measured values.

Compound	***Exact Mass***	***3+***	***4+***	***5+***	***6+***
Molecular Weight (g/mol)	2846.48	2847.60	2847.80	2848.55	2846.94

CRA_DV_3023

The spectrum for the compound is showed in Figure 24, where can be seen fragments from 4+ to 6+. Focusing on Table 11, the obtained molecular weight of the different fragments displayed in the spectrum were very resembling. This indicated that the CRA_DV_3023 glycopeptide corresponded to the designed compound.

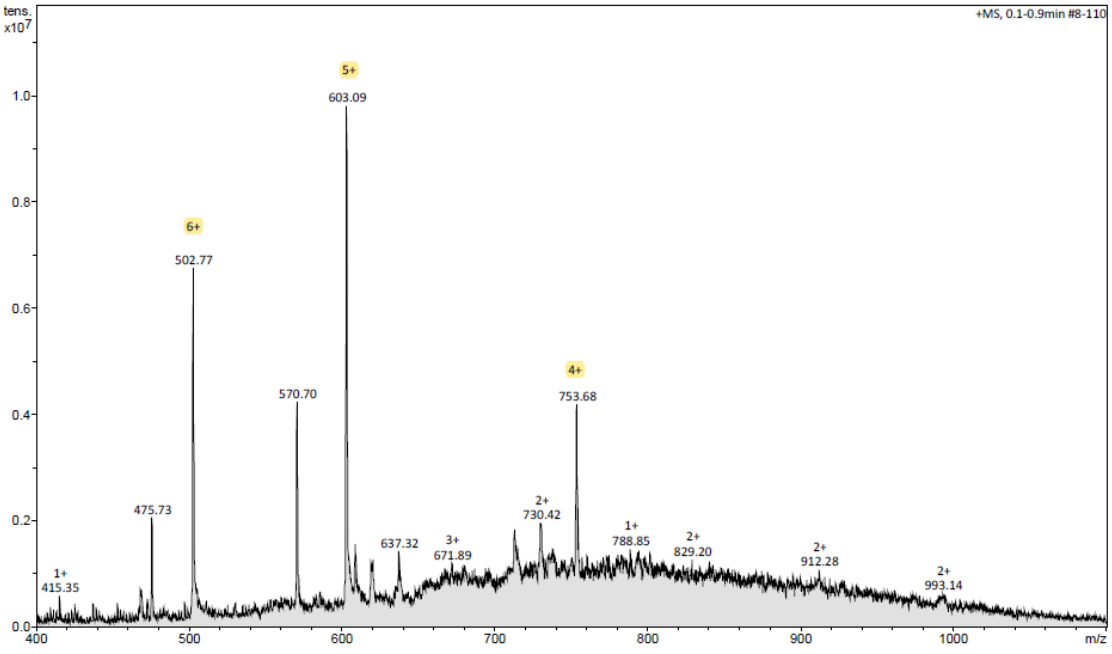

Figure 24. ESI-MS spectrum for CRA_DV_3023.

Table 11. Comparison between the calculated molecular weight of CRA_DV_3023 with the measured values.

Compound	*Exact Mass*	*4+*	*5+*	*6+*
Molecular Weight (g/mol)	3008.54	3010.72	3010.45	3010.62

CRA_DV_3024

The displayed spectrum for CRA_DV_3024 in Figure 25, contain multiply charged molecules from 3+ to 6+. Looking at Table 12, the results of the molecular weight of the charged molecules are very similar to the exact mass calculated for the compound, concluding that the synthesized compound corresponded to the desired glycopeptide.

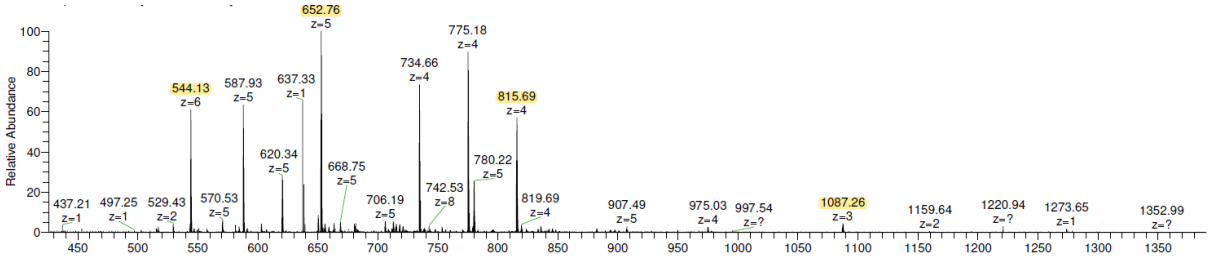

Figure 25. ESI-MS spectrum for CRA_DV_3024.

Table 12. Comparison between the calculated molecular weight of CRA_DV_3022 with the measured values.

Compound	*Exact Mass*	*3+*	*4+*	*5+*	*6+*
Molecular Weight (g/mol)	3257.62	3258.78	3258.76	3258.80	3258.78

CRA_TG_3025

The mass spectrum for the compound is displayed in Figure 26, where charged molecules from 3+ to 5+ can be observed. Now looking at Table 13, the results of the measured molecular weight are very similar to the exact mass calculated for the glycopeptide, concluding that the synthesized CRA_TG_3025 corresponded to the desired compound.

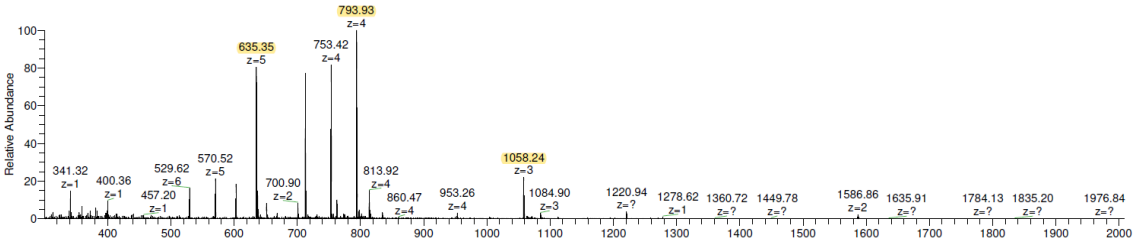

Figure 26. ESI-MS spectrum for CRA_DV_3025.

Table 13. Comparison between the calculated molecular weight of CRA_DV_3023 with the measured values.

Compound	***Exact Mass***	***3+***	***4+***	***5+***
Molecular Weight (g/mol)	3170.59	3171.72	3171.72	3171.75

After referring to the characterization results of all the compounds, the conclusion is that all the compounds correspond to the desired glycopeptides, stating the favorable outcome of not only the ESI-MS characterization, but also the success in the correct synthesis of the designed peptides by SPPS, and the purification step by preparative HPLC. All this shows the success of the experimental part of the thesis.

6. CONCLUSION

As discussed before, the initial objectives of this Bachelor's Thesis were to successfully synthesize four glycopeptides (all containing different carbohydrate motifs), and after that, to correctly assess the purification by preparative HPLC, obtaining pure substances. After that, a crucial step would be the characterization by ESI-MS of these glycopeptides to demonstrate the identity of the compounds to continue with further investigation.

Regarding the synthesis of the compounds, all the steps described in the experimental part of the thesis were carried out without major problems. The only setback encountered during the synthesis was a malfunction in the coupling program of the Prelude® automatic synthesizer, which could be assessed by fixing its configuration, and only delayed the process for one day. The preparation of the used coupling, deprotection, and cleavage solutions also was carried out without any complication.

The purification process by preparative HPLC was also a success because the total amount of the purified peptides (from which the yield is calculated), did not decrease the amount of product obtained enough to affect the correct development of the peptide characterization, amount that in the case of a positive characterization would also allow the correct conduction of the programmed *in vitro* and *in vivo* studies to test the properties of the compounds. The positive results can be also observed in the obtention of the pure compounds in all the cases, as can be seen in the mostly narrow peaks of the HPLCs measured.

Now focusing on the characterization of the compounds synthesized and purified by ESI-MS, all the molecular weights calculated from the multiply charged compounds in the spectra obtained from the measurement of the pure peptide samples, showed very similar results compared to the previously calculated molecular weights of the designed compounds, concluding that all the compounds assessed corresponded to the desired compounds.

All these facts support the success of the steps detailed in the experimental part of this Bachelor's Thesis. These positive results will lead to the development of *in vitro* and *in vivo* studies, which, due to the large period of time that need to be carried out, are not included in this thesis.

Last of all, I would like to thank all the Polt research group for all their help and their kindness. The working environment in the laboratory has been very pleasant, and all the members of the group met me with open arms. For this awesome experience I need to specially thank Christopher Apostol, who has made my stay in the US very fulfilling. He did not only mentor me and helped me whenever I needed, but he was also very nice and supportive since the first day. This experience has been very rewarding and a once in a lifetime opportunity to expand my knowledge in a lot of different areas.

7. BIBLIOGRAPHY

[1] Lamine, A.; Poujol de Molliens, M.; Létourneau, M.; Hébert, T. E.; Vaudry, D.; Fournier, A.; Chatenet, D. The Amidated PACAP1-23 Fragment Is a Potent Reduced-Size Neuroprotective Agent. Biochim. Biophys. Acta Gen. Subj. 2019, 1863 (11), 129410.

[2] Bourgault, S.; Chatenet, D.; Wurtz, O.; Doan, N. D.; Leprince, J.; Vaudry, H.; Fournier, A.; Vaudry, D. Strategies to Convert PACAP from a Hypophysiotropic Neurohormone into a Neuroprotective Drug. Curr. Pharm. Des. 2011, 17 (10), 1002–1024.

[3] Sherwood, N. M.; Krueckl, S. L.; McRory, J. E. The Origin and Function of the Pituitary Adenylate Cyclase-Activating Polypeptide (PACAP)/Glucagon Superfamily. Endocr. Rev. 2000, 21 (6), 619–670.

[4] Huang, M.; Shirahase, H.; Rorstad, O. P. Comparative Study of Vascular Relaxation and Receptor Binding by PACAP and VIP. Peptides 1993, 14 (4), 755–762.

[5] Lindén, A.; Yoshihara, S.; Chan, B.; Nadel, J. A. Inhibition of Bronchoconstriction by Pituitary Adenylate Cyclase Activating Polypeptide (PACAP 1-27) in Guinea-Pigs in Vivo. Br. J. Pharmacol. 1995, 115 (6), 913–916.

[6] Seaborn, T.; Masmoudi-Kouli, O.; Fournier, A.; Vaudry, H.; Vaudry, D. Protective Effects of Pituitary Adenylate Cyclase-Activating Polypeptide (PACAP) against Apoptosis. Curr. Pharm. Des. 2011, 17 (3), 204–214.

[7] Gervais, F. G.; Xu, D.; Robertson, G. S.; Vaillancourt, J. P.; Zhu, Y.; Huang, J.; LeBlanc, A.; Smith, D.; Rigby, M.; Shearman, M. S.; Clarke, E. E.; Zheng, H.; Van Der Ploeg, L. H.; Ruffolo, S. C.; Thornberry, N. A.; Xanthoudakis, S.; Zamboni, R. J.; Roy, S.; Nicholson, D. W. Involvement of Caspases in Proteolytic Cleavage of Alzheimer's Amyloid-Beta Precursor Protein and Amyloidogenic A Beta Peptide Formation. Cell 1999, 97 (3), 395–406.

[8] Mei, Y. A.; Vaudry, D.; Basille, M.; Castel, H.; Fournier, A.; Vaudry, H.; Gonzalez, B. J. PACAP Inhibits Delayed Rectifier Potassium Current via a CAMP/PKA Transduction Pathway: Evidence for the Involvement of I k in the Anti-Apoptotic Action of PACAP. Eur. J. Neurosci. 2004, 19 (6), 1446–1458.

[9] Botia, B.; Basille, M.; Allais, A.; Raoult, E.; Falluel-Morel, A.; Galas, L.; Jolivel, V.; Wurtz, O.; Komuro, H.; Fournier, A.; Vaudry, H.; Burel, D.; Gonzalez, B. J.; Vaudry, D. Neurotrophic Effects of PACAP in the Cerebellar Cortex. Peptides 2007, 28 (9), 1746–1752.

[10] Shioda S.; Ohtaki H.; Suzuki R.; Nakamachi T.; Takenoya F.; Dohi K.; Nakajo S. Prevention of delayed neuronal cell death by PACAP and its molecular mechanism. Nihon Yakurigaku Zasshi 2004, 123 (4), 243–252.

[11] Malishkevich, A.; Marshall, G. A.; Schultz, A. P.; Sperling, R. A.; Aharon-Peretz, J.; Gozes, I. Blood-Borne Activity-Dependent Neuroprotective Protein (ADNP) Is Correlated with Premorbid Intelligence, Clinical Stage, and Alzheimer's Disease Biomarkers. J. Alzheimers. Dis. 2016, 50 (1), 249–260.

[12] Kinney, J. W.; Bemiller, S. M.; Murtishaw, A. S.; Leisgang, A. M.; Salazar, A. M.; Lamb, B. T. Inflammation as a Central Mechanism in Alzheimer's Disease. Alzheimers Dement. (N. Y.) 2018, 4 (1), 575–590.

[13] Fuster, J. J.; Walsh, K. The Good, the Bad, and the Ugly of Interleukin-6 Signaling. EMBO J. 2014, 33 (13), 1425–1427.

[14] Bourgault, S.; Vaudry, D.; Guilhaudis, L.; Raoult, E.; Couvineau, A.; Laburthe, M.; Ségalas-Milazzo, I.; Vaudry, H.; Fournier, A. Biological and Structural Analysis of Truncated Analogs of PACAP27. J. Mol. Neurosci. 2008, 36 (1–3), 260–269.

[15] Neuroscientifically Challenged. Know your brain: Blood-brain barrier.

https://www.neuroscientificallychallenged.com/blog/know-your-brain-blood-brain-barrier#:~:text=The%20blood%2Dbrain%20barrier%20acts,extracellular%20space%20of%20the%20brain.&text=In%20other%20blood%20vessels%20throughout,spaces%20and%20into%20surrounding%20tissues.

(accessed Jun 8, 2021).

[16] Bobbi Lynn Anglin. Design and Synthesis of PACAP Based Glycopeptide Analogs; Effects of Glycosylation on Activity and Blood-Brain Barrier Penetration; The University of Arizona; Tucson, AZ, 2014.

[17] Lalatsa, A.; Butt, A. M. Physiology of the Blood–Brain Barrier and Mechanisms of Transport across the BBB. In Nanotechnology-Based Targeted Drug Delivery Systems for Brain Tumors; Elsevier, 2018; pp 49–74.

[18] Blood-brain barrier & the spinal cord - blog

https://www.christopherreeve.org/blog/research-news/blood-brain-barrier-the-spinal-cord

(accessed Jun 17, 2021).

[19] Kubotera, H.; Ikeshima-Kataoka, H.; Hatashita, Y.; Allegra Mascaro, A. L.; Pavone, F. S.; Inoue, T. Astrocytic Endfeet Re-Cover Blood Vessels after Removal by Laser Ablation. Sci. Rep. 2019, 9 (1), 1263.

[20] Daneman, R.; Zhou, L.; Kebede, A. A.; Barres, B. A. Pericytes Are Required for Blood-Brain Barrier Integrity during Embryogenesis. Nature 2010, 468 (7323), 562–566.

[21] Brown, L. S.; Foster, C. G.; Courtney, J.-M.; King, N. E.; Howells, D. W.; Sutherland, B. A. Pericytes and Neurovascular Function in the Healthy and Diseased Brain. Front. Cell. Neurosci. 2019, 13, 282.

[22] Muoio, V.; Persson, P. B.; Sendeski, M. M. The Neurovascular Unit - Concept Review. Acta Physiol. (Oxf.) 2014, 210 (4), 790–798.

[23] Li, Y.; Lefever, M. R.; Muthu, D.; Bidlack, J. M.; Bilsky, E. J.; Polt, R. Opioid Glycopeptide Analgesics Derived from Endogenous Enkephalins and Endorphins. Future Med. Chem. 2012, 4 (2), 205–226.

[24] Pardridge, W. M. The Blood-Brain Barrier: Bottleneck in Brain Drug Development. NeuroRx 2005, 2 (1), 3–14.

[25] Thermo Fisher. Protein Glycosylation

https://www.thermofisher.com/es/es/home/life-science/protein-biology/protein-biology-learning-center/protein-biology-resource-library/pierce-protein-methods/protein-glycosylation.html

(accessed Jun 10, 2021)

[26] Green, B. D.; Irwin, N.; Flatt, P. R. Pituitary Adenylate Cyclase-Activating Peptide (PACAP): Assessment of Dipeptidyl Peptidase IV Degradation, Insulin-Releasing Activity and Antidiabetic Potential. Peptides 2006, 27 (6), 1349–1358.

[27] Palian, M. M.; Boguslavsky, V. I.; O'Brien, D. F.; Polt, R. Glycopeptide-Membrane Interactions: Glycosyl Enkephalin Analogues Adopt Turn Conformations by NMR and CD in Amphipathic Media. J. Am. Chem. Soc. 2003, 125 (19), 5823–5831.

[28] Jones, E. M.; Polt, R. CNS Active O-Linked Glycopeptides. Front. Chem. 2015, 3, 40.

[29] Li, Y.; St Louis, L.; Knapp, B. I.; Muthu, D.; Anglin, B.; Giuvelis, D.; Bidlack, J. M.; Bilsky, E. J.; Polt, R. Can Amphipathic Helices Influence the CNS Antinociceptive Activity of Glycopeptides Related to β-Endorphin? J. Med. Chem. 2014, 57 (6), 2237–2246.

[30] 50% of what? How exactly are IC50 and EC50 defined?

https://www.graphpad.com/support/faq/50-of-what-how-exactly-are-ic50-and-ec50-defined/

(accessed Jun 10, 2021).

[31] Lowery, J. J.; Yeomans, L.; Keyari, C. M.; Davis, P.; Porreca, F.; Knapp, B. I.; Bidlack, J. M.; Bilsky, E. J.; Polt, R. Glycosylation Improves the Central Effects of DAMGO. Chem. Biol. Drug Des. 2007, 69 (1), 41–47.

[32] Jaradat, D. M. M. Thirteen Decades of Peptide Synthesis: Key Developments in Solid Phase Peptide Synthesis and Amide Bond Formation Utilized in Peptide Ligation. Amino Acids 2018, 50 (1), 39–68.

[33] Guillier, F.; Orain, D.; Bradley, M. Linkers and Cleavage Strategies in Solid-Phase Organic Synthesis and Combinatorial Chemistry. Chem. Rev. 2000, 100 (6), 2091–2158.

[34] Chemical Book. β-D-Glucose Pentaacetate. https://www.chemicalbook.com/ChemicalProductProperty_EN_CB4217013.htm (accessed Jun 14, 2021).

[35] Sigma-Aldrich. Fmoc-Ser-OH. https://www.sigmaaldrich.com/catalog/product/aldrich/47601?lang=en&region=US (accessed Jun 14, 2021).

[36] Fmoc-Ser-OBn https://www.chembk.com/en/chem/Fmoc-Ser-OBn (accessed Jun 14, 2021).

[37] Lactose octaacetate

https://www.sigmaaldrich.com/ES/es/product/aldrich/772356

(accessed Jun 14, 2021).

[38] Solving Aspartimide Formation in Fmoc SPPS with Fmoc-Asp(OBno)-OH

https://www.sigmaaldrich.com/ES/es/technical-documents/technical-article/chemistry-and-synthesis/peptide-synthesis/overcoming-aspartimide-formation

(accessed Jun 14, 2021).

[39] Siuzdak, G. An Introduction to Mass Spectrometry Ionization: An Excerpt from The Expanding Role of Mass Spectrometry in Biotechnology, 2nd Ed.; MCC Press: San Diego, 2005. J. Lab. Autom. 2004, 9 (2), 50–63.